THE UNIVERSITY OF CHICAGO

OPPOSING MOTOR MEMORIES IN THE DIRECT AND INDIRECT PATHWAYS OF THE BASAL GANGLIA

A DISSERTATION SUBMITTED TO

THE FACULTY OF THE DIVISION OF THE BIOLOGICAL SCIENCES

AND THE PRITZKER SCHOOL OF MEDICINE

IN CANDIDACY FOR THE DEGREE OF

DOCTOR OF PHILOSOPHY

COMMITTEE ON NEUROBIOLOGY

BY

KAILONG WEN

CHICAGO, ILLINOIS

JUNE 2024

To My Family

TABLE OF CONTENTS

LIST OF FIGURES.....vii

LIST OF ABBREVIATIONS.....ix

ABSTRACT xi

CHAPTER 1 INTRODUCTION 1

1.1 Basal ganglia anatomy 1

1.2 Functional studies of basal ganglia..... 3

1.3 *in vivo* recording of basal ganglia activity 5

1.4 D2 pathway's role in learning and memory 7

1.5 Parkinson's Disease and Aberrant Inhibitory Learning..... 8

1.5 Overview 11

CHAPTER 2 OPPOSING MOTOR MEMORIES IN THE DIRECT AND INDIRECT PATHWAYS OF THE BASAL GANGLIA..... 13

2.1 Abstract..... 13

2.2 Introduction 14

2.3 Results 16

2.3.1 Memory of normal learning is preserved after aberrant inhibitory learning . 16

2.3.2 dSPN and iSPN striatal neuron activities during normal and aberrant inhibitory learning..... 21

2.3.3 Dissociation of D1 pathway-dependent normal learning and D2 pathway-dependent inhibitory learning..... 30

2.3.4 Computational Model supports preserved memory of normal learning in direct pathway after inhibitory learning 34
2.4 Discussion 38
2.5 Method 43
2.5.1 Transgenic mice 43
2.5.2 Mouse Rotarod Behavior 44
2.5.3 Drug Administration 44
2.5.4 Stereotaxic Surgery 44
2.5.5 Fiber photometry 45
2.5.6 Neuronal culture 46
2.5.7 Click chemistry 46
2.5.8 Quantification and statistical analysis 47
2.5.9 Computational model 47
2.6 Author Contributions 47
2.7 Acknowledgements 48
2.8 Declaration of Interests 48
2.9 Supplementary Figures 48
CHAPTER 3 NEURAL PATHWAYS AND MOLECULAR MECHANISMS IN NORMAL AND ABERRANT INHIBITORY LEARNING 55
3.1 Abstract 55
3.2 Introduction 55
3.3 Results 57
3.3.1 Exploring cFos Expression in Normal and Inhibitory Learning (WT) 57

3.3.2 Exploring cFos Expression in Normal and Inhibitory Learning (Pitx3 mutant) 60

3.3.3 Investigating the cAMP pathway via DREADDs in normal and inhibitory learning 63

3.3.4 β-arrestin is not required for inhibitory learning 68

3.3.5 D2 receptor is required for normal learning process 69

3.3.6 Rescue of aberrant inhibitory learning by D1 agonist 70

3.3.7 Erasing aberrant inhibitory learning through normal learning process (WT mice) 72

3.4 Discussion 74

3.5 Method 77

3.5.1 Transgenic mice 77

3.5.2 Rotarod 77

3.5.3 Open field 78

3.5.4 Drug Administration 78

3.5.5 Immunostaining 78

3.5.6 Quantification and statistical analysis 79

CHAPTER 4 DISCUSSION 80

4.1 Tag and capture in the basal ganglia: A hypothesis 80

4.2 Direct and indirect pathways mediate positive and negative reward prediction error 82

4.3 Increased iSPN activity at movement initiation 83

4.4 Aberrant inhibitory learning vs. extinction learning 84

4.5 m6A, synaptic plasticity, and memory consolidation 85

4.6 Conclusion 86

REFERENCE 88

LIST OF FIGURES

Fig 2.1. Memory of normal learning was preserved after aberrant inhibitory learning, whereas inhibitory memory was reversed by normal learning……..…17

Fig 2.2. Fiber photometry recording of dSPNs and iSPNs in dorsal striatum during normal motor learning……..22

Fig 2.3. Preserved memory of normal learning after aberrant inhibitory learning was reflected in the activities of dSPNs……..26

Fig 2.4. Ythdf1 gene deletion experiments showed double dissociation and suggested that normal learning and inhibitory learning are mediated mainly by the D1 and D2 pathways respectively……32

Fig 2.5. Modeling dopamine effects on mice rotarod performance under various experimental conditions…….……35

Fig S2.1. Individual trial data for different rotarod experiments…….…….49

Fig S2.2. PCA analysis of fiber photometry signal……..51

Fig S2.3. Measuring new protein synthesis in Ythdf1 KO using Click chemistry……52

Fig S2.4. Computational model describing rotarod motor learning and performance in mice with conditional Ythdf1 gene deletion in A2a Cre mice……54

Fig 3.1. Neuronal activity in normal and aberrant inhibitory motor learning (WT mice)…….58

Fig 3.2. Neuronal activity in normal and aberrant inhibitory motor learning (Pitx3 -/- mice)……..……..61

Fig 3.3. Chemogenetic studies on normal and aberrant inhibitory learning……..……65

Fig 3.4. Signaling pathways in normal and aberrant inhibitory learning……..69

Fig 3.5. Rescue of aberrant inhibitory learning by D1 agonist and prolonged normal learning process……..71

LIST OF ABBREVIATIONS

SNr	substantia nigra pars reticulata
GPi	internal segment of the globus pallidus
GPe	globus pallidus externus
DMS	dorsomedial striatum
VMS	ventromedial striatum
VLS	ventrolateral striatum
RPE	reward prediction error
dSPN	direct spiny projection neuron
iSPN	indirect spiny projection neuron
CaCaM	calcium/calmodulin
AC5	adenylyl cyclase type 5
HFS	High-frequency stimulation protocol
WT	wild type
CHX	cycloheximide
PKA	protein kinase A
M1	primary motor cortex
M2	secondary motor cortex
DREADDs	Designer Receptors Exclusively Activated by Designer Drugs
D2 Kd	D2 dopamine receptor knockdown
PD	Parkinson’s disease
e-LTP	early long-term plasticity

l-LTP	late long-term plasticity

ABSTRACT

Loss of dopamine neurons causes motor deterioration in Parkinson's disease patients. We have previously reported that in addition to acute motor impairment, the impaired motor behavior is encoded into long-term memory in an experience-dependent and task-specific manner, a phenomenon we refer to as aberrant inhibitory motor learning.

Although normal motor learning and aberrant inhibitory learning oppose each other and this is manifested in apparent motor performance, in the present study, we found that memory of normal motor learning acquired prior to aberrant inhibitory learning remains preserved in the brain, suggesting the existence of independent storage. To investigate the neuronal circuits underlying these two opposing memories, we took advantage of the RNA-binding protein YTHDF1, an m^6A RNA methylation reader involved in the regulation of protein synthesis and learning/memory. Conditional deletion of *Ythdf1* in either D1 or D2 receptor-expressing neurons revealed that memory of normal learning is stored in the D1 (direct) pathway of the basal ganglia, while inhibitory memory is stored in the D2 (indirect) pathway. Furthermore, fiber photometry recordings of GCaMP signals from striatal D1 (dSPN) and D2 (iSPN) receptor-expressing neurons support the preservation of memory in normal learning in the direct pathway after aberrant inhibitory learning, with activities of dSPN predictive of motor performance. We also built a computational model based on activities of motor cortical neurons, dSPN and iSPN neurons, and their interactions through the basal ganglia loops that successfully explained various experimental observations.

Building on the computational model, we investigated the neuronal population underlying normal and aberrant inhibitory learning via cFos expression, and studied the role of intracellular cAMP pathway in aberrant inhibitory learning using chemogenetic approaches. Finally, we explored potential approaches for rescuing and reversing aberrant inhibitory learning, and we found that D1 agonist treatment or prolonged normal learning could rescue aberrant inhibitory learning in mice.

Together, these findings have important implications for novel approaches in treating Parkinson's disease by reactivating preserved memory of normal learning, and in treating hyperkinetic movement disorders such as chorea or tics by erasing aberrant motor memories.

CHAPTER 1 INTRODUCTION

1.1 Basal ganglia anatomy

The basal ganglia, a subcortical structure in the brain, plays a crucial role in many functions, including motor control, cognition, and the regulation of emotions. Dysfunctions within this region are linked to various neurological disorders, such as Parkinson's disease, Huntington's disease, and substance use disorders. The basal ganglia includes striatum, pallidum, subthalamic nucleus, and substantia nigra, and it receives cortical inputs and projects to the thalamus, forming the cortico-striatal-thalamic loop. The development of advanced imaging and tracing technologies in recent years has shed light on the detailed anatomy of this loop, enhancing our understanding of its complex mechanisms.

The cortico-striatal-thalamic loop includes two pathways: the direct pathway, mediated by medium spiny neurons (MSNs) expressing dopamine D1 receptors, and the indirect pathway, characterized by MSNs expressing dopamine D2 receptors. The direct pathway facilitates inputs from the cortex and thalamus directly to the basal ganglia's output nuclei—the substantia nigra pars reticulata (SNr) and the internal segment of the globus pallidus (GPi). Conversely, the indirect pathway projects to globus pallidus externus (GPe), which then projects to the SNr and GPi. Research has shown that activation of D1-expressing MSNs in the direct pathway results in the excitation of cortical areas, whereas activation of D2-expressing MSNs in the indirect pathway

inhibits cortical activity[1]. These opposite effects establish a dynamic balance within the cortico-striatal-thalamic loop, with the D1 pathway contributing to a positive feedback loop and the D2 pathway creating a negative feedback loop. Such an arrangement ensures balanced regulation of motor and cognitive functions.

Given the large area of cortex and striatum, the relationship between different cortical regions and their corresponding basal ganglia projections have been heavily investigated. Garrett E. Alexander's seminal proposal of five parallel loops through the striatum and thalamus laid the foundation for us to understand these intricate connections[2]. Subsequent research has confirmed the existence of these parallel loops, indicating a conserved anatomical relationship that persists throughout the basal ganglia network[3]. The direct and indirect pathways split their routes when they project out from the striatum, but the indirect pathway eventually reconverges with the direct pathway in SNr/GPi by sending projection from the GPe to SNr/GPi. With detailed tracing and mapping, we now know that direct and indirect pathways originating from the same sub-striatal domain ultimately re-converge onto the same postsynaptic SNr neurons, further strengthening the parallel loop model[4,5].

Moreover, the interactions between these loops are facilitated by distinct mechanisms, as evidenced by early primate studies showing striato-nigral-striatal and thalamo-cortical-thalamic crosstalks[6]. Recent findings by the Jin Group extend our understanding by uncovering a unidirectional influence of the limbic system over motor functions mediated through a circuit linking the ventral striatum, substantia nigra (SNr),

and motor thalamus[7]. This discovery provides new evidence on how emotional and motivational states can affect motor outputs.

In addition to crosstalk at the circuit level, another form of crosstalk between D1 and D2 pathways could happen at the synaptic level. Electron microscopy studies reveal that individual cortical or thalamic terminals can simultaneously form synapses with both direct and indirect pathway MSNs, suggesting a potential site for cross-pathway communication[8]. Despite the need for further research to quantify the prevalence of cortical inputs innervating both direct and indirect pathways, existing evidence points to a significant overlap in their innervation. This is further illustrated by in vivo calcium imaging data showing coactivity among dSPNs and iSPNs within the striatum, as long as the neuronal population are spatially close[9].

Together, past research on basal ganglia anatomy highlights the complex connections between direct and indirect pathways and loops in different subregions. We next examine the research effort to understand the function of basal ganglia.

1.2 Functional studies of basal ganglia

The advent of optogenetic techniques, together with the development of BAC transgenic mice models expressing Cre recombinase specifically in D1-expressing medium spiny neurons (D1 Cre) or D2-expressing MSNs (A2a Cre), has advanced our understanding of the basal ganglia's role in motor control. Optogenetic manipulation of these pathways has provided direct evidence of their differential influence on behavior: activation of the

D1 pathway facilitates movement, whereas stimulation of D2 MSNs results in movement inhibition[10]. This dichotomy is further supported by studies showing that D1/D2 activation respectively augments or diminishes cortical activity, offering direct insight into the basal ganglia circuitry's influence on motor behaviors[1,11].

In addition to activating a large population of dSPNs or iSPNs, activation within specific striatal subregions has been shown to elicit distinct motor functions. For instance, stimulation of the dorsomedial striatum (DMS) and ventromedial striatum (VMS) can induce contralateral turning, while targeted activation of the ventrolateral striatum (VLS) leads to contralateral licking[11]. Such findings underscore the striatum's complex role in coordinating diverse motor responses, suggesting that different striatal regions modulate specific aspects of motor function based on their unique projection targets outside the basal ganglia[3].

Building on the past results, recent investigations in rats have further shown the striatum's critical contribution to motor memory storage. Contrary to the idea that cortical regions are responsible for storing learned memories, it has been demonstrated that the striatum is essential for retaining learned motor patterns[12]. Lesions within the striatum, but not the cortex, effectively erased previously acquired motor skills, highlighting the striatum's role in motor memory consolidation.

Together, these functional studies not only affirm the basal ganglia's central role in motor control and learning but also reveal the complex interplay between different

neuronal pathways and subregions within this brain structure. To understand how these pathways facilitate movement and motor learning *in vivo*, we next discuss findings from *in vivo* recording in the basal ganglia.

1.3 *in vivo* recording of basal ganglia activity

The development of *in vivo* recording techniques capable of monitoring the activity of D1 and D2 neurons in freely moving animals has significantly advanced our understanding of basal ganglia function. Early experiments in the striatum revealed that both D1 and D2 neurons increase their activity at the onset of operant learning and just before movement initiation, while showing reduced activity during periods of immobility[13]. This evidence challenged the traditional **rate model**, which proposed that D1 and D2 neurons have opposing roles in movement, with D1 increasing and D2 decreasing during movement.

Supported by early optogenetic studies[10], the rate model suggested that selective activation of D2 neurons could induce freezing and diminish movement initiation, whereas D1 neuron activation could decrease freezing and enhance locomotor activities. This model was challenged with research using more sophisticated task designs and temporal optogenetic manipulations, showing that both D1 and D2 pathways are crucial for a balanced action initiation and execution sequence[14]. These results support the **selection-suppression** model, where the D1 pathway aids in choosing and initiating actions, and the D2 pathway plays a more permissive role in

inhibiting undesired actions within the same context. Interestingly, as learning progresses, striatal activity patterns evolve, as evidenced by fiber photometry studies showing a decline in striatal activity with improved performance on tasks like the accelerating rotarod[15].

The introduction of GRIN lens microscopes has enabled the observation of D1 and D2 neuronal activity within the same animal at a cellular resolution[9]. A study found that dSPNs and iSPNs showed high co-activity during the course of movement as long as they are spatially close within the striatum. This led to the emergence of a **spatiotemporal selection model**, where D1 and D2 neurons coordinate to select motor programs, showing greater similarity and proximity when encoding for the same type of movement compared to different movements[9]. However, the study is limited by not involving any learning component during the recording, as the experiments were conducted in open field tests. Indeed, desynchronized activity patterns between D1 and D2 neurons have been observed in experiments involving cocaine-induced place preference, suggesting that their coactivity may vary under conditions involving learning and memory[16].

Overall, while different models propose varying roles for dSPNs and iSPNs in motor control and learning, there is a consensus that these striatal neurons encode a motor action space, exhibiting distinct activity patterns during different actions[17]. This evolving understanding illustrates the complexity of the striatum's role in encoding and executing motor functions.

1.4 D2 pathway's role in learning and memory

Both dSPNs and iSPNs are modulated by dopamine signaling, with D1 receptors positively coupled to downstream cAMP signaling while D2 receptors negatively coupled. Because of this difference, they respond differently to change in dopamine activity in the brain and are involved in different aspects of learning and memory[18–20].

Extensive research has shown that dopamine signaling represents a reward prediction error (RPE) in the brain, which is the difference between received and predicted future rewards[21,22]. In the reward prediction model, an increase or decrease in dopamine firing represents positive and negative reward prediction errors, respectively. One prevalent hypothesis is that D2 receptors are responsible for detecting negative reward prediction errors. Supporting this hypothesis, several studies have shown that D2 receptors play a key role in reversal learning mediated by negative RPE[23–26]. Early primate studies showed that the dopamine D2 antagonist raclopride significantly impaired reversal learning but not new skill acquisition, while the D1/D5 receptor antagonist SCH 23390 did not significantly modulate acquisition of a novel discrimination nor reversal learning[26]. Similar results were also reported in mice pharmacology studies[24]. In addition to pharmaco-genetic manipulations, several mouse genetic studies also reported that D2 receptor deficient mice showed a delay in reversal learning and were inflexible in changing their behavior when the environment changed[23,25].

Another example of learning mediated by negative RPE is aversive learning. Studies have shown that D2 receptor mediated activation of PKA is key in the formation and retention of aversive memories[20,27]. Additionally, recent studies also have shown direct evidence that the D2 receptor underlies the detection of dopamine firing decrease and the following enlargement of dendritic spines during discrimination learning[28]. These studies have shown that the D2 pathway is important in detecting negative reward prediction errors and mediating the corresponding learning process, which are essential for animal survival. On the other hand, the D2 pathway is also involved in learning and memory underlying pathological conditions, such as Parkinson's disease and Huntington's disease.

1.5 Parkinson's Disease and Aberrant Inhibitory Learning

Neurodegeneration of dopamine neurons causes Parkinson's disease in human patients. The main symptoms involved in PD are unintended or uncontrollable movements, such as shaking, stiffness, and difficulty with balance and coordination.

The canonical explanation for PD symptoms is the hyperactive D2 pathway caused by dopamine loss. According to the classic model of basal ganglia function[2,10,29,30], activity in the D1 receptor-expressing, direct 'Go' pathway increases excitation of cortical activity and facilitates movement. By contrast, activity in the D2 receptor-expressing, indirect 'No-Go' pathway, inhibits cortical activity and movement. At the cellular level, activation of dopamine receptors on striatal neurons modulates the gating of ion

channels and, therefore, acutely alters the intrinsic excitability of these neurons[31–33]. Thus, neurodegeneration of dopamine neurons will cause a hypoactive D1 pathway and hyperactive D2 pathway, which leads to the inhibition of movement and motor coordination.

However, in addition to the modulation of intrinsic excitability, dopamine also modulates corticostriatal plasticity in both the direct and indirect pathways[34–38]. With this second mechanism, dopamine, or the lack of dopamine is able to produce cumulative and long-lasting changes in corticostriatal synapses. These synaptic changes ensure a persistent impairment of motor function[39–41].

The contribution of aberrant corticostriatal synaptic plasticity to PD motor symptoms has been highlighted by multiple studies in recent years[37,39,41–46]. This is distinct from the traditional view that denervation of dopamine neurons causes an imbalance between the direct and indirect pathways and impairs motor performance acutely[29,30]. We have shown in animal models that the combination of dopamine deficiency and motor experience leads to aberrant corticostriatal LTP in the indirect pathway. As a consequence, there develops an experience-dependent and task-specific gradual increase in motor inhibition and a deterioration of motor performance, a “use it and lose it” phenomenon[39,43–46]. This framework fits with the cellular level functions of dopamine in modulating corticostriatal plasticity[34–38]. At a behavioral level, responses that are reinforced by dopamine will be selected more in the future whereas responses that are not reinforced by dopamine will be inhibited in the future[39,47]. Task specificity

corresponds to the fact that corticostriatal plasticity in specific synapses is dependent on specific cortical glutamatergic inputs at that time.

Mechanistically, both the dopamine D1 and D2 receptors are strongly coupled to the cAMP pathway[48,49]. Dopamine primarily stimulates cAMP production in D1 receptor expressing neurons and inhibits cAMP production in D2 receptor expressing neurons. The striatum is unique in the expression of the calcium/calmodulin (CaCaM)-insensitive adenylyl cyclase type 5 (AC5)[50–52]. This is distinct from other brain regions such as the hippocampus and cortex that express predominantly the CaCaM-activated cyclase, AC1[53–55]. There is little or no AC1 expression in the adult striatum[50–52]. Therefore, cAMP production in adult striatum is highly modulated by G-protein coupled receptors rather than by calcium, and this may explain why dopamine signaling plays such a dominant role in the induction and directionality of corticostriatal plasticity[36–38,56]. Studies, including ours, suggest that the direction and magnitude of plasticity in D2 neurons are regulated by both the afferent activity and D2 neuron intracellular cAMP. High concentrations of dopamine reduce cAMP via D2 receptor activation and facilitate LTD in the indirect pathway[56–58]. In contrast, low dopamine levels increase intracellular cAMP, favoring LTP in the indirect pathway[37,56]. In mice lacking D2 receptors, high-frequency stimulation protocol (HFS) that would normally induce LTD instead induced LTP[59]. In 6-OHDA lesioned mice, a model of PD, HFS induced corticostriatal LTD in the indirect pathway was impaired[42]. Therefore, when dopamine levels decrease as PD progresses, it favors corticostriatal LTP induction in the indirect “NoGo” pathway and facilitates the gradual development of motor inhibition.

1.5 Overview

As this thesis delves into the phenomenon of aberrant inhibitory learning, we aim to address several questions across the following chapters. Chapter 2 explores the relationship between normal motor learning and aberrant inhibitory learning. Through a combination of behavior, pharmacology, genetic modifications, and in vivo recording techniques, we aim to investigate the underlying mechanisms of these learning processes. Additionally, we have constructed a computational model that seeks to explain the observed behavioral phenotypes through dopamine's role in modulating cAMP-dependent signaling pathways.

In Chapter 3, we focus on identifying the specific neuronal populations that underlying the normal and aberrant inhibitory learning, and further investigate the role of cAMP signaling in these learning paradigms, using both chemogenetic and genetic methodologies. Through these approaches, we try to understand the neural circuits and signaling mechanisms that underlies normal and aberrant inhibitory motor learning, providing insights that extend beyond Parkinson's disease to a broader neurobiological principle.

In essence, this thesis aims to bridge gaps in our understanding of motor learning, utilizing various techniques to uncover the complex interplay between normal and aberrant inhibitory learning. We anticipate uncovering novel insights that will not only

enrich our understanding of the basal ganglia's role in learning and memory but also inform future research directions and therapeutic strategies for addressing neurological disorders such as PD.

CHAPTER 2 OPPOSING MOTOR MEMORIES IN THE DIRECT AND INDIRECT PATHWAYS OF THE BASAL GANGLIA

2.1 Abstract

Loss of dopamine neurons causes motor deterioration in Parkinson's disease patients. We have previously reported that in addition to acute motor impairment, the impaired motor behavior is encoded into long-term memory in an experience-dependent and task-specific manner, a phenomenon we refer to as aberrant inhibitory motor learning. Although normal motor learning and aberrant inhibitory learning oppose each other and this is manifested in apparent motor performance, in the present study, we found that memory of normal learning acquired prior to aberrant inhibitory learning remains preserved in the brain, suggesting the existence of independent storage. To investigate the neuronal circuits underlying these two opposing memories, we took advantage of the RNA-binding protein YTHDF1, an m^6A RNA methylation reader involved in the regulation of protein synthesis and learning/memory. Conditional deletion of *Ythdf1* in either D1 or D2 receptor-expressing neurons revealed that memory of normal learning is stored in the D1 (direct) pathway of the basal ganglia, while inhibitory memory is stored in the D2 (indirect) pathway. Furthermore, fiber photometry recordings of GCaMP signals from striatal D1 (dSPN) and D2 (iSPN) receptor-expressing neurons support the preservation of memory in normal learning in the direct pathway after aberrant inhibitory learning, with activities of dSPN predictive of motor performance. Finally, a computational model based on activities of motor cortical neurons, dSPN and iSPN

neurons, and their interactions through the basal ganglia loops supports the above observations. These findings have important implications for novel approaches in treating Parkinson's disease by reactivating preserved memory of normal learning, and in treating hyperkinetic movement disorders such as chorea or tics by erasing aberrant motor memories.

2.2 Introduction

The dopamine system and the basal ganglia play unique roles in motor control and motor learning.[60,61] The D1 and D2 dopamine receptors are expressed in two distinct pathways: the D1 (direct) and D2 (indirect) pathways.[33,62] Despite their well-recognized roles in facilitating and inhibiting movement,[10,63,64] how each of these pathways contributes to learning processes and how they are involved in memory storage, particularly under pathological conditions, remain largely underexplored.

In Parkinson's disease (PD), degeneration of dopamine neurons in the substantia nigra leads to significant disruptions in the balance between the D1 (direct) and D2 (indirect) pathways.[9,65] We have previously reported that in addition to acute motor impairment caused by dopamine loss or dopamine receptor blockade, the impaired motor behavior is contributed largely by motor experience-dependent gradual deterioration of motor performance in the absence of dopamine receptor activation, a "use it and lose it" phenomenon we refer to as aberrant inhibitory motor learning.[43,44,46]

Aberrant Inhibitory learning reminds us of the concept of extinction learning; both processes are experience dependent and task specific, and lead to a decline in previously acquired responses. In extinction learning, the formation of extinction memory doesn't necessarily erase the original memory; rather, it superimposes a new memory that opposes the behavioral level expression of the initial memory (For review, see [66,67]). The similarities between extinction learning and aberrant inhibitory learning prompted us to ask: does aberrant inhibitory learning erase memory of normal learning? In other words, are memory of normal learning and aberrant inhibitory memory stored independently or even in separate anatomical pathways?

Our earlier studies suggest that aberrant inhibitory learning is mediated by the D2 (indirect) pathway.[43] We therefore examined if memory of normal learning and aberrant inhibitory memory are stored independently in the D1 (direct) and D2 (indirect) pathways respectively. We used behavioral designs to specifically probe normal motor learning versus aberrant inhibitory motor learning, and recorded GCaMP signals from D1 and D2 receptor-expressing dSPNs and iSPNs. In order to use manipulations to selectively impair, therefore dissociate, normal learning and aberrant inhibitory learning, we used a genetic approach by deleting the *Ythdf1* gene in dSPNs or iSPNs. Many studies have shown that new protein synthesis is required for long-term memory formation. YTHDF1 is an m^6A RNA methylation reader protein, a specific RNA-binding protein that recognizes and binds to m^6A modified mRNAs and facilitates their translation.[68] It has been shown that it works with FMRP and plays a significant role in

synaptic plasticity, learning and memory.[69,70] Collectively, our behavioral, GCaMP recording and genetic data all support our hypothesis that memory of normal learning and aberrant inhibitory memory are stored independently in the D1 (direct) and D2 (indirect) pathways respectively. Finally, we built a computational model based on activities of motor cortical neurons, D1 and D2 receptor-expressing neurons, and their interactions through the basal ganglia loops and validated the above hypothesis.

2.3 Results

2.3.1 Memory of normal learning is preserved after aberrant inhibitory learning

We used our previously established approach to study the relationship between aberrant inhibitory learning and normal motor learning in wild type (WT) mice and Pitx3 mutant mice using an accelerating rotarod task (Figure 2.1A). Consistent with our previous report, WT mice trained on rotarod under dopamine antagonists treatment showed impaired behavior even after the washout of the drug (Figure 2.1B, two-way ANOVA on day 8-9, group effect, $F(1, 13) = 13.25$, $p = 0.0030$; group x time interaction $F(1, 13) = 7.829$, $p = 0.0151$). In the experiment, the mice (red group) during aberrant inhibitory learning showed stereotyped immobile behavior on the rotarod. This immobile behavior persisted when we re-exposed them to the rotarod task even after the dopamine antagonists were washed out (probe phase).

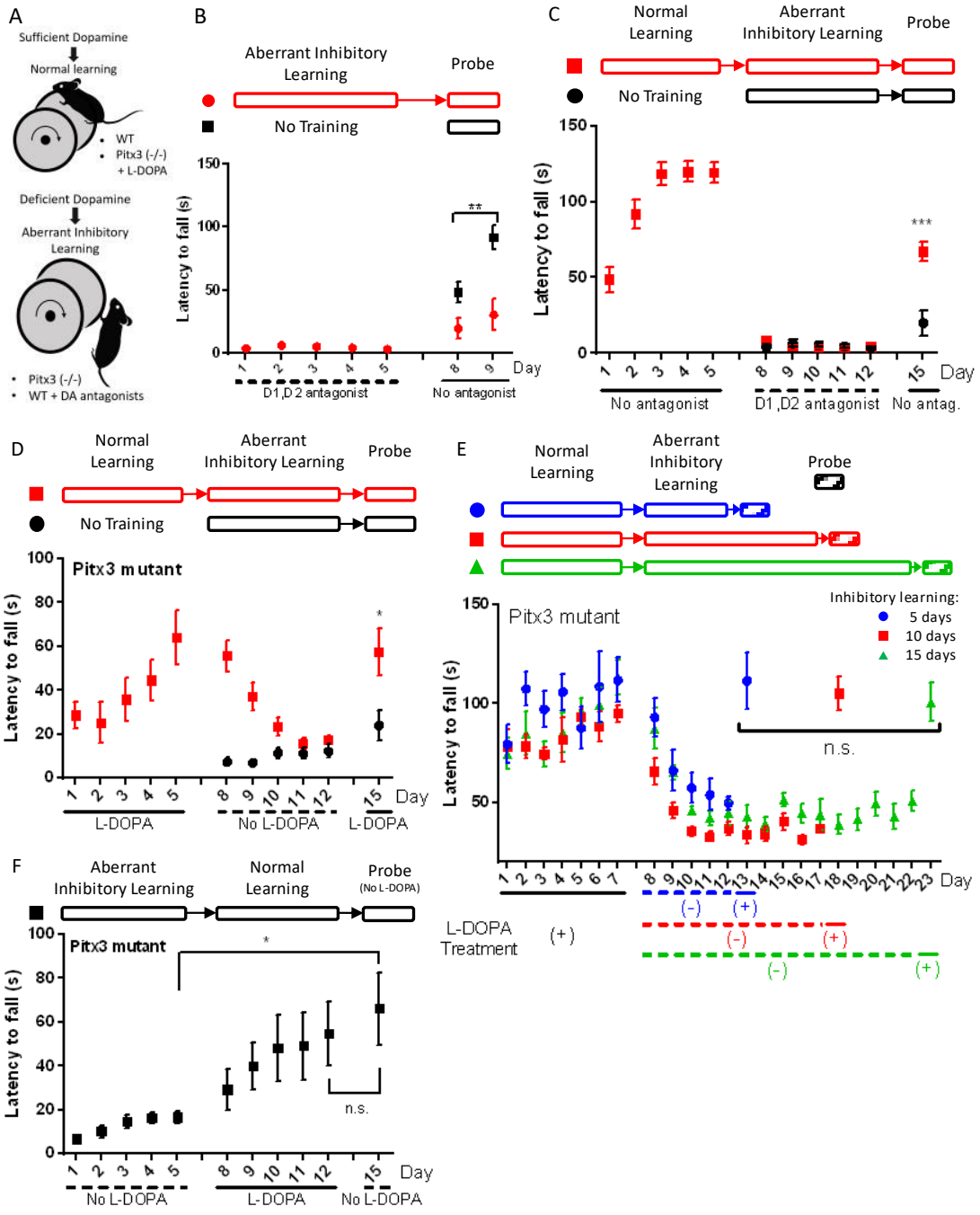

Fig 2.1. Memory of normal learning was preserved after aberrant inhibitory learning, whereas inhibitory memory was reversed by normal learning.

(A) Experimental designs for normal motor learning (WT mice without drug treatment or Pitx3 mutant mice treated with L-DOPA) and inhibitory motor learning (WT mice treated with dopamine antagonists or Pitx3 mutant mice without L-DOPA treatment).

Fig. 2.1 cont.

(B) Dopamine antagonist cocktail (SCH22390 and Eticlopride) treatment induced long-term impairment even after drug washout. Two-way ANOVA on day 8-9, group effect, $F(1, 13) = 13.25$, $p = 0.0030$; group x time interaction $F(1, 13) = 7.829$, $p = 0.0151$, $n = 8$ for each group.

(C) In WT mice (red group) with previous normal learning experience showed significantly better performance in probe phase compared to the control (black) group. t test on day 15, $p=0.0006$, $n = 7$ for black group, $n = 8$ for red group. (antag., antagonist)

(D) In Pitx3 mutant mice (red group) with previous normal learning experience showed significantly better performance in probe phase than the control (black) group, indicating preserved memory of normal learning. t test on day 15, $p=0.0251$, $n = 6$ for each group.

(E) In Pitx3 mutant mice, memory of normal learning was equally preserved after 5, 10 or 15 days of inhibitory learning. One-way ANOVA of rotarod performance on L-DOPA treated days between 13 (blue), 18 (red) and 23 (green) day, $F(2, 17) = 0.255$, $p = 0.778$. $n = 6$ for the blue group with 5 days of inhibitory learning; $n = 7$ for the red group with 10 days of inhibitory learning; $n = 7$ for the green group with 15 days of inhibitory learning.

(F) Pitx3 mutant mice showed sustained improvement from aberrant inhibitory learning after normal learning experience, indicating inhibitory memory was reversed. One-way ANOVA between day 5, 12, and 15, day effect $F(2, 21) = 4.124$, $p = 0.0308$. Post-hoc Tukey HSD test, Day 15 vs Day 5, $p = 0.031$, day 15 vs day12, $p = 0.794$, $n= 8$.

All data represents mean ± SEM. *, $p<0.05$; **, $p<0.01$; ***, $p<0.001$. n.s., not significant.

To investigate whether inhibitory motor learning erases memory of normal learning, we designed a three-phase motor learning paradigm involving motor skill learning on an accelerating rotarod using WT mice (Figure 2.1C, top). In the normal learning phase, only one group was trained on rotarod to acquire memory of normal learning, while the other group received no training. In the aberrant inhibitory learning phase, both groups were treated with dopamine D1 (SCH22390) and D2 (Eticlopride) antagonist cocktails and trained on the rotarod. This procedure induced aberrant inhibitory learning in both groups and they both showed a performance deficit as expected. In the probe phase,

both groups were tested under no drug condition on rotarod. This three-phase experiment allowed us to test if memory of normal learning is preserved after inhibitory learning. To our surprise, we found that during the probe phase, the group with previous normal learning experience showed significantly better performance than the control group (Figure 2.1C and S2.1A-C; 2.1C, t test on day 15, P=0.0006). These data suggest that memory of normal learning acquired before inhibitory learning is still preserved after inhibitory learning.

Next, we tested the same hypothesis using the Pitx3 deficient mutant mice that lack the nigrostriatal dopaminergic pathway throughout development.[71] The experiment was similarly designed with three-phases (Figure 2.1D, top). One group of Pitx3 deficit mice went through normal learning (L-DOPA treatment), aberrant inhibitory learning (no L-DOPA) and probe phase (L-DOPA treatment). The second group of Pitx3 deficit mice went through only aberrant inhibitory learning and the probe phase. In normal learning phase, consistent with what we reported before,[44] L-DOPA treated Pitx3 deficit mice successfully acquired the rotarod motor skill (Figure 2.1D). When both groups of mice were trained without L-DOPA during the aberrant inhibitory learning phase, the mice with normal learning experience showed a gradual decline of the motor performance, and the control mice showed low performance. Both groups reached the same level of low performance at the end of the aberrant inhibitory learning phase. In the probe phase, both groups were tested on rotarod again under L-DOPA condition. Remarkably, the group with previous normal learning experience showed significantly better performance than the control group (Figure 2.1D and S2.1D-F; 2.1D, t test on day 15, P=0.0251). These data indicate that the memory of normal learning is still preserved in

the Pitx3 deficit mice even after aberrant inhibitory learning.

To rigorously assess the durability of the preserved memory of normal learning in Pitx3 deficit mice, we used the three-phase behavior design with different lengths of aberrant inhibitory learning (Figure 2.1E, top). All three groups of Pitx3 mutant mice were trained with L-DOPA in the normal learning phase to form the memory of normal learning, and then they went through 5, 10, or 15 days of rotarod training without L-DOPA (aberrant inhibitory learning phase). Next, they were tested under L-DOPA condition to determine the extent to which memory of normal learning had been retained (probe phase). Surprisingly, we found that all three groups showed similar levels of recovery in probe phase (Figure 2.1E and S2.1G-H; 2.1E, one-way ANOVA on probe phase, $F(2, 17) = 0.255$, $P = 0.778$). This observation suggests that the preserved memory of normal learning in these models is resilient to extended periods of dopaminergic deficiency and aberrant inhibitory learning.

Since memory of normal learning is preserved after the aberrant inhibitory learning process, is the inhibitory memory also resistant to normal learning process? To test that, we designed another three-phase experiment using Pitx3 deficit mice. Mice were trained on an ‘aberrant inhibitory learning - normal learning - probe’ schedule (Figure 2.1F, top). The first two phases were intended to induce aberrant inhibitory memory and memory of normal learning respectively. As expected, mice performance improved over days during the normal learning phase. Then mice were tested without L-DOPA on the probe phase. If the aberrant inhibitory memory was not reversed by the normal learning experience, we expected to see a similar performance between the aberrant inhibitory

learning phase and the probe phase. To our surprise, the rotarod performance during probe phase did not show a sharp drop to the performance level of aberrant inhibitory learning (Figure 2.1F and S2.1I-J; One-way ANOVA between day 5,12, and 15, day effect p= $F(2, 21) = 4.124$, $P = 0.0308$; post-hoc Tukey HSD test, Day 15 vs Day 5, $p = 0.031$). On the contrary, the rotarod performance without L-DOPA treatment (probe phase) was maintained at a similar level as the end of normal learning phase (Figure 2.1F and S2.1I-J; post-hoc Tukey HSD test, day 15 vs day12, $p = 0.794$). These data suggest that inhibitory memory can be reversed by normal learning.

2.3.2 dSPN and iSPN striatal neuron activities during normal and aberrant inhibitory learning

To examine if the preserved memory of normal learning after aberrant inhibitory learning is reflected in activities of direct (dSPN) or indirect (iSPN) spiny projection neuron in the dorsal striatum, and to further characterize the neuronal activities during normal and aberrant inhibitory learning, we performed *in vivo* fiber photometry recording of Ca2+ activities during our rotarod motor learning paradigm. Previous studies had shown that dorsal striatum is important for rotarod motor learning.[15,72–74] We injected a Cre-dependent GCaMP6m AAV9 into the dorsal striatum in either D1-Cre mice or A2a-Cre mice (Figure 2.2A, B) to express the calcium activity sensor in either the dSPN or iSPN respectively. We used the three-phase design described above (Figure 2.2C).

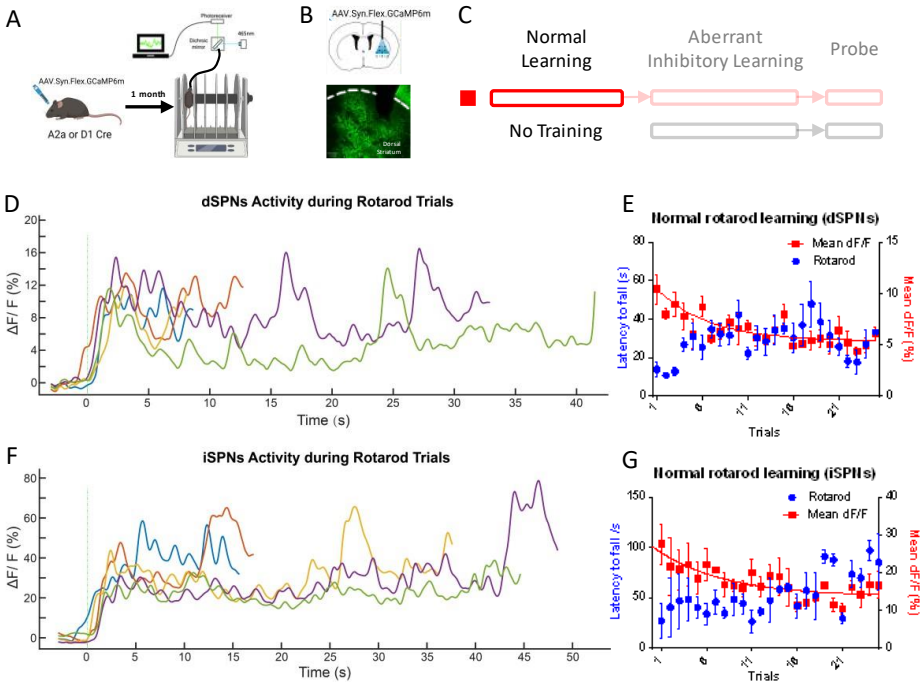

Fig 2.2. Fiber photometry recording of dSPNs and iSPNs in dorsal striatum during normal motor learning.

(A) Experimental design for fiber photometry recording of Ca^{2+} activity in dorsal striatum during rotarod motor learning task. AAV-mediated dSPNs and iSPNs expression of GCaMP6m was achieved after local injection of Cre recombinase-dependent AAV into the dorsal striatum of D1-Cre and A2a-Cre transgenic mice respectively.

(B) Top, schematic of injection site and optical fiber placement (black bar) for the GCaMP6m Ca^{2+} sensor. Bottom, fluorescence image showing GCaMP6m (green). White dashed line, border of striatum. Fiber placed between the tissue gap of dashed lines. Fiber placement position (AP +0.7, ML +2.25, depth 2.6mm).

(C) The three-phase experimental design used for fiber photometry recordings.

(D-G) Fiber photometry recordings during normal motor learning.

(D) Representative traces of Ca^{2+} signal in dSPNs during rotarod test. Each trace is a single trial, with green dash line indicating the beginning of a trial.

Fig. 2.2 cont.

(E) Mean Ca^{2+} activity in dSPNs throughout the rotarod motor skill acquisition phase, n = 4. One-phase exponential decay in mean Ca2+ signal following rotarod training, fitted using the equation Y=(10.39 - 5.35)*exp(-0.169*X) + 5.35, half-life = 4.1, time constant = 5.92, R^2 = 0.28. Mean ± SEM.

(F) Representative traces of Ca^{2+} signal in iSPNs during rotarod test.

(G) Mean Ca^{2+} activity in D2 striatal neurons throughout the rotarod motor skill acquisition phase, n = 3. One-phase exponential decay in mean Ca2+ signal following rotarod training, fitted using the equation Y=(26.85 - 13.61)*exp(-0.13*X) + 13.61, half-life = 5.25, time constant =7.58, R^2 =0.24. Mean ± SEM.

During the normal motor learning phase, we found that both dSPN and iSPN calcium signals showed an increase at the beginning of the rotarod trial and stayed elevated throughout the trial (Figure 2.2D, F). Interestingly, as the mice learned the rotarod over several days, the average amplitude of the Ca2+ signal in both dSPN and iSPN gradually decreased (Figure 2.2E, G; 2.2E, One-phase exponential decay, Y=(10.39 - 5.35)*exp(-0.169*X) + 5.35, half-life = 4.1, time constant = 5.92, R^2 = 0.28; 2.2G, One-phase exponential decay, Y=(26.85 - 13.61)*exp(-0.13*X) + 13.61, half-life = 5.25, time constant =7.58, R^2 =0.24). This seems to suggest both the direct and indirect pathways are involved in normal motor learning. However, it is important to keep in mind that both direct and indirect pathways could change during motor learning, but they are not necessarily the mechanisms underlying motor learning.

We next studied the neuronal activities during aberrant inhibitory learning phase (Figure 2.3B, and 2.3C-J), where we treated mice with a dopamine antagonist cocktail (SCH22390 and Eticlopride). The mice under dopamine antagonists treatment had

stereotyped immobile behavior on the rotarod, and this behavior persisted when the mice were re-exposed to the rotarod context even after the dopamine antagonists were washed out. To understand the neuronal activity underlying the immobile behavior (aberrant inhibitory learning), we divided the trials into short (<5s, mostly immobile behavior) and long (>10s) trials. When we examined the distribution of trial length in the two groups, we found that the group with previous normal learning experience had fewer short trials compared with the group not previously trained (Figure 2.3C, G). This is true for the later probe phase as well (see below and Figure 2.3K, O). In studying fiber photometry signals during the aberrant inhibitory learning phase, we aligned the start of the trial between long and short trials to understand the neuronal activity that contributed to the short trials. We found that there is no difference between short and long trials in the dSPN signal, in either group (Figure 2.3D, E). This observation is further confirmed when we compared the mean Ca2+ signal of the first 2 seconds of the trials. Neither trial length nor group factor is significant in a mixed effects model (Figure 2.3F. Mixed effect model, trial length factor, $p = 0.50$; group factor, $p=0.92$). Next, we looked at fiber photometry signals in the indirect pathway during the aberrant inhibitory learning phase. There is no difference between short and long trials in the group with previous normal learning experience (Figure 2.3H). However, we found that in the short trials of the control group, iSPN signal sharply increased after the beginning of the trial (Figure 2.3I). When comparing the mean signal of the first 2s of the trial, the iSPN signal in the short trial of the control group showed a trend of higher value comparing with the rest of the group, though not statistically significant (Figure 2.3J. Mixed effect model, trial length factor, $p=0.39$; group factor, $p = 0.47$). However, the group with normal

learning experience earlier seemed more protected from such an effect. These data suggest that higher iSPN signal is associated with poor performance during aberrant inhibitory learning, which is consistent with the idea of a hyperactive indirect pathway during aberrant inhibitory learning, although it is conceivable that normal activities of iSPN and appropriate level of inhibition are necessary for normal learning as well.

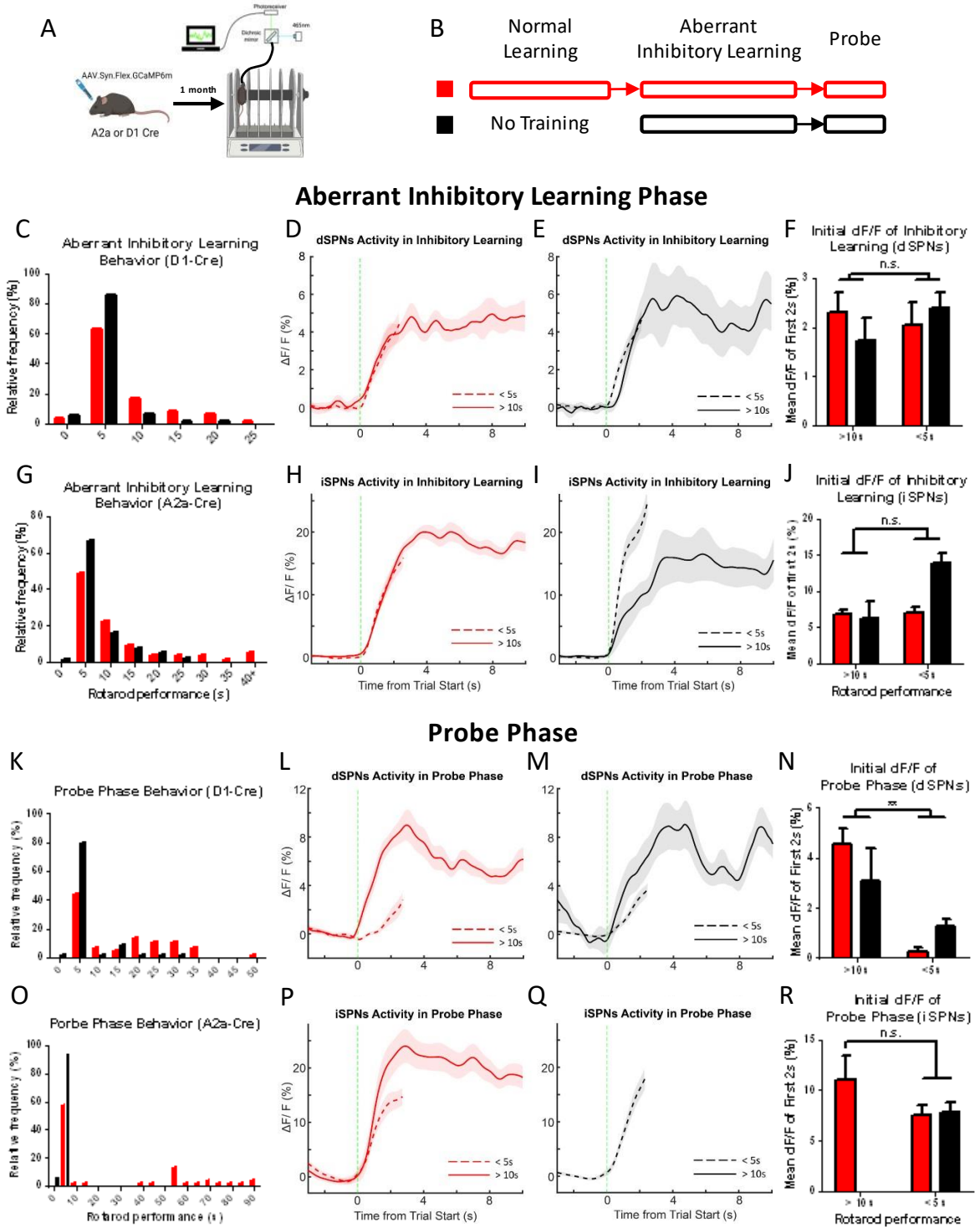

Fig 2.3. Preserved memory of normal learning after aberrant inhibitory learning was reflected in the activities of dSPNs

Fig 2.3. cont.

(A) Fiber photometry recording setup.

(B) Experimental design for fiber photometry recording of Ca^{2+} activity in dorsal striatum during aberrant inhibitory learning and probe phase (Normal learning phase is shown in figure 2). Red group was trained in normal learning phase while black group did not receive normal motor learning.

(C-J) Fiber photometry recordings during aberrant inhibitory learning phase.

(C) Histogram of rotarod behavior during the aberrant inhibitory learning phase of mice used in dSPNs recordings.

(D) Mean dSPNs Ca^{2+} signal of the red group (with previous normal learning experience) during aberrant inhibitory learning. Dashed line, < 5s trials; solid line, > 10s trials. Mean ± SEM.

(E) Same as (D) but for the black group with no previous normal learning experience.

(F) Comparing mean dSPNs Ca^{2+} signal of the first 2s of the aberrant inhibitory learning phase between red and black groups (with or without previous normal learning experience). There was a total of 43 trials from 3 red group mice and 53 trials from 3 black group mice. Mixed effect model, trial length factor, $p = 0.50$; group factor, $p=0.92$. Mean ± SEM.

(G-J) Same as (C-F) but for iSPNs recordings.

(I) In the black group without previous normal learning, higher iSPNs activities predict shorter trials. Mean ± SEM.

(J) Comparing mean iSPNs Ca^{2+} signal of the first 2s between red and black groups. There was a total of 57 trials from 3 red group mice and 52 trials from 3 black group mice. Mixed effect model, trial length factor, $p=0.39$; group factor, $p = 0.47$.

(K-R) Same as (C-J) but for the probe phase of the fiber photometry experiment.

(L) In the red group with previous normal learning experience, lower dSPNs activities predict shorter trials. Mean ± SEM.

(M) In black group with no previous normal learning experience, lower dSPNs activities also predict shorter trials. Mean ± SEM.

(N) Comparing mean dSPNs Ca^{2+} signal of the first 2s between red and black groups (with or without previous normal learning experience). There was a total of 43 trials from 3 red group mice and 43 trials from 3 black group mice. Mixed effect model, trial length factor, $p = 0.0019$; group factor, $p=0.92$. Mean ± SEM.

(R) Comparing mean iSPNs Ca^{2+} signal of the first 2s between red and black group. There was a total of 42 trials from 3 red group mice and 45 trials from 3 black group mice. Mixed effect model, trial length factor, p=0.43; group factor, p = 0.65. Mean ± SEM.

*, p<0.05; **, p<0.01. n.s., not significant.

After dopamine antagonist induced aberrant inhibitory learning, all the groups are tested under the drug-free condition (Figure 2.3B and 2.3K-R, probe phase). Again, when we examined the distribution of trial length in different groups, we found that trials in the group with previous normal learning showed less distribution in the short trials compared with the control group, consistent with our behavior studies (Figure 2.3K, 2.3O and S2.1C). Similar to the above analysis in the aberrant inhibitory learning phase, we divided the trials into long (>10s) and short (<5s) trials. In the fiber photometry signal, we found that the dSPN signal in short trials showed a slower ramp compared with the long trials (Figure 2.3L, M). This observation was consistent in both groups with or without previous normal learning experience, and was further confirmed by the significantly higher average signal of the first 2 seconds of the long trials (Figure 2.3N. Mixed effect model, trial length factor, p = 0.0019; group factor, p=0.92). The fiber photometry signals in the indirect pathway showed a similar trend of difference between long and short trials but were not statistically significant (Figure 2.3R. Mixed effect model, trial length factor, p=0.43; group factor, p = 0.65). These data suggest that a faster activity ramp in the D1 pathway is associated with better performance. Given that the group with previous normal learning has more long trials with a faster activity ramp in the D1 pathway compared with the control group, we conclude that previous normal

training experience before aberrant inhibitory learning induced higher dSPN activity during the drug-free probe phase, potentially an underlying mechanism for their better performance in the probe phase.

To examine whether there are similarities in fiber photometry signals between the normal learning phase and the probe phase, we performed principal component analysis (PCA) (Figure S2.2) using several features extracted from each individual trial in the two phases (when performance was not under drug influence). The photometry signal features we used in PCA include: signal peak rate, trial signal mean, trial standard deviation, signal mean during trial beginning, and signal mean during trial end. In analysis of the dSPN fiber photometry data, principal components 1 and 2 successfully explained 82.0% and 12.5% of the total variance respectively. When we plotted all the trials together using principal component 1 and 2, we observed a clustering pattern in which there is a clear separation between the normal learning phase and the probe phase data from the group without previous normal learning (Figure S2.2B). However, the probe phase data from the group with previous normal learning (recall of normal learning) overlaps with normal learning phase and with probe phase data from the group without previous normal learning, potentially suggesting that the group with previous normal learning showed features of both the memory of normal learning and aberrant inhibitory memory during the probe phase. Similarly, we performed such PCA analysis on iSPN fiber photometry data, principal component 1 and 2 explained 84.0% and 10.9% of the variance respectively. However, when we plotted all the trials using PC1 and PC2, the iSPN data from the normal learning phase and the probe phase were mixed and did not show a clear clustering pattern (Figure

S2.2C).

2.3.3 Dissociation of D1 pathway-dependent normal learning and D2 pathway-dependent inhibitory learning

Our earlier studies suggest that inhibitory motor learning is mediated by the D2 (indirect) pathway.[43] The present fiber photometry data suggest that activities in the D1 (direct) pathway is more important for normal motor learning, which is in agreement with previously reported optogenetic inhibition studies.[72] To further investigate the roles of D1 and D2 pathways in normal and aberrant inhibitory motor memory , we designed a double dissociation experiment utilizing conditional *Ythdf1* gene deletion. Previous studies showed that *Ythdf1* gene deletion impaired new protein synthesis, synaptic plasticity in the hippocampus and hippocampus-dependent learning.[70] To confirm the role of YTHDF1 in regulating new protein synthesis in the striatum, we measured the new protein synthesis rate using click chemistry technology in primary striatal neuronal culture.[75–77] Specifically, we incubated the striatal neuronal culture with a methionine analog HPG in a methionine free medium to label the newly synthesized protein, and later tagged the HPG with fluorophore using click chemistry reaction for visualization. We found that the fluorescence intensity was much higher in the baseline group compared with a negative control group, where we treated cells with cycloheximide (CHX), a protein translation inhibitor (Figure 2.4A, B and S2.3A. One-way ANOVA, $F(2,99)=97.7$, $P<0.0001$; post hoc Tukey HSD test, ‘CHX’ vs ‘Baseline’, Q statistic = 5.54, $P=0.001$). After validation of the method, we treated cells with forskolin to activate adenylyl cyclase and its downstream signaling as an approach to activate intracellular

protein synthesis. We saw that forskolin treatment significantly increased HPG signal, which indicated higher protein synthesis rate (Figure 2.4A, B and S2.3A. Post hoc Tukey HSD test ‘Baseline’ vs ‘Forskolin’, Q statistic = 12.88, P=0.001). Surprisingly, when we performed the same procedure in the striatal neurons derived from *Ythdf1* knockout, they did not show such an increased protein translation when cells are treated with forskolin (Figure 2.4A, C and S2.3B. T-test ‘Baseline’ vs ‘Forskolin’, $p<0.0001$). On the contrary, striatal neurons from the *Ythdf1* knockout showed a much higher baseline protein translation rate than the neurons in WT. This result suggests that *Ythdf1* KO striatal neurons are impaired in activating protein translation in response to extracellular stimuli. While it is conceivable that cells that do not respond to elevated activities by elevating protein synthesis rate need to have a higher baseline protein translation rate in order to sustain normal cellular functions with sufficient protein translation activities, the consequences of elevated baseline protein translation rate are worth investigating in the future. Of note, the higher protein synthesis rate caused by

stimulation is far lower than the maximum limit of our assay, ruling out a ceiling effect.

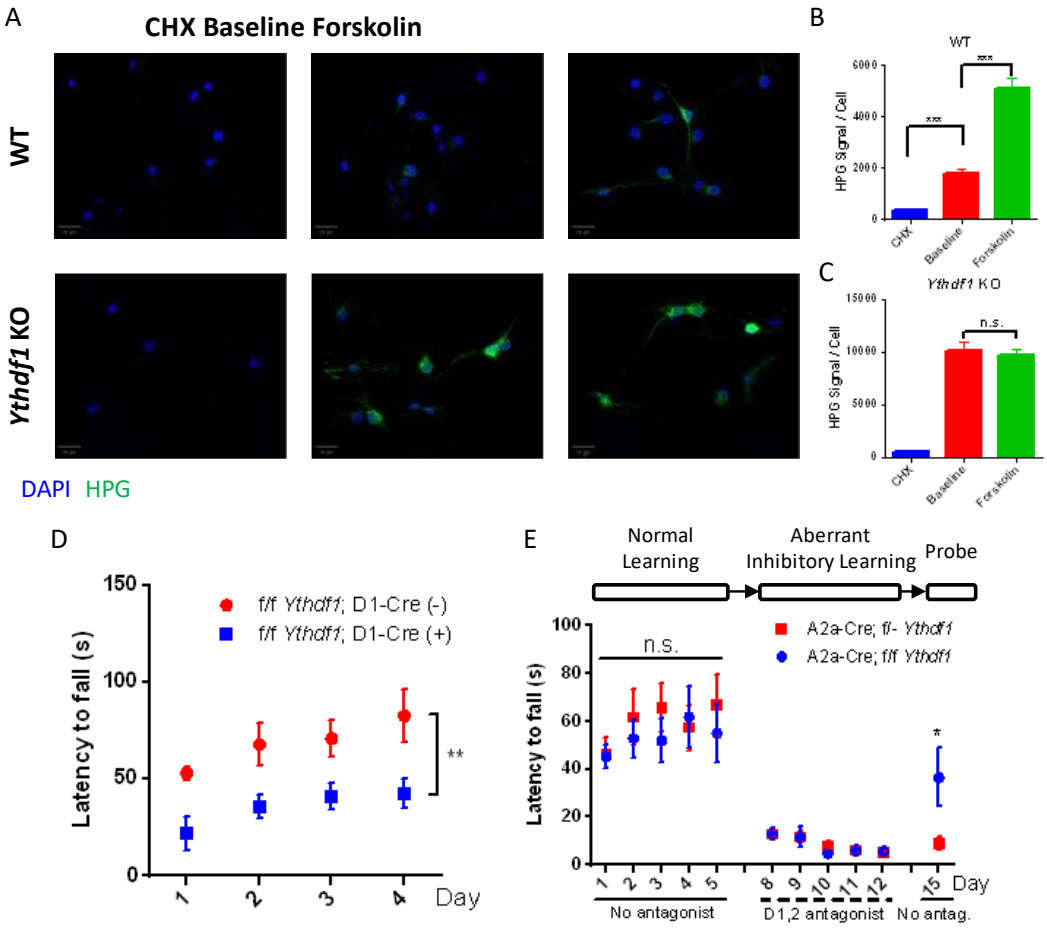

Fig 2.4. *Ythdf1* gene deletion experiments showed double dissociation and suggested that normal learning and inhibitory learning are mediated mainly by the D1 and D2 pathways respectively.

(A) Representative merged images of click chemistry experiment measuring protein synthesis rate in WT and *Ythdf1* KO mice. Blue, DAPI staining; green, HPG tagged newly synthesized protein. Scale bar, 20 μm. CHX, Cycloheximide.

(B) Quantification of newly synthesized protein during CHX, baseline and forskolin treatment in WT striatal neurons. One-way ANOVA, $F(2,99)=97.7$, $P<0.0001$; post hoc Tukey HSD test, 'CHX' vs 'Baseline', Q statistic = 5.54, p=0.001; 'Baseline' vs 'Forskolin', Q statistic = 12.88, p=0.001.

(C) Quantification of newly synthesized protein during CHX, baseline and forskolin

Fig 2.4. cont.

treatment in *Ythdf1* KO striatal neurons. Student t-test 'Baseline' vs 'Forskolin', p=0.6927. n= 36 for CHX, and Forskolin group, n= 30 for HPG group. Each group contains 3 replicates.

(D) Conditional gene deletion of *Ythdf1* in D1-Cre mice led to an impairment in the normal motor learning paradigm. Two-way ANOVA, group effect F(1, 12) =11.23, p= 0.0058. Group x time interaction F(3, 36) = 0.2895, p=0.8327. n= 7 for each group.

(E) Conditional gene deletion of *Ythdf1* in A2a-Cre mice led to similar normal motor learning but more protection against aberrant inhibitory motor learning compared to the control group. Two-way ANOVA on day 1-5, group effect F(1, 9) =0.2586, p=0.6233. Group x time interaction F(4, 36) = 0.8894, p=0.4802. t-test on day 15, p=0.0398. n(A2a Cre x f/f *Ythdf1*) = 5. n(A2a Cre x f/- *Ythdf1*) = 6.

All data represent mean ± SEM. *, p<0.05; **, p<0.01; ***, p<0.001. n.s., not significant.

After validating the role of YTHDF1 in regulating protein synthesis in the striatum. We deleted *Ythdf1* in the D1 or D2 pathway. We hypothesize that impaired new protein synthesis in dSPN or iSPN should impair D1 or D2 pathway dependent learning respectively. We first tested whether the D1 pathway is important for normal motor learning using D1 neuron specific *Ythdf1* gene deletion (D1-Cre x floxed-*Ythdf1)* and control mice of 6 months. We found that rotarod performance during normal learning was significantly impaired in mutant mice compared to controls (Figure 2.4D. Two-way ANOVA, group effect F(1, 12) =11.23, P= 0.0058; group x time interaction F(3, 36) = 0.2895, P=0.8327). Because the normal learning was already impaired in D1-Cre x floxed-*Ythdf1* mice, this prevented us from further testing if they were impaired in inhibitory learning.

Next, we investigated the involvement of the D2 pathway of the basal ganglia in normal

and inhibitory learning. Using A2a-Cre mouse line crossed with floxed-*Ythdf1*, we generated mice with conditional deletion of *Ythdf1* in D2 dopamine receptor-expressing cells. We found that 6-month-old mutant mice showed no difference during normal learning compared with the controls (Figure 2.4E. Two-way ANOVA on day 1-5, group effect $F(1, 9) = 0.2586$, $P=0.6233$; group x time interaction $F(4, 36) = 0.8894$, $P=0.4802$), suggesting that new protein synthesis in the D2 pathway is not directly involved in normal motor learning. To investigate whether the aberrant inhibitory learning is affected, we trained mice on rotarod under dopamine D1 & D2 antagonist cocktails, and then tested both groups without drug injection (Figure 2.4E, top). We found that conditional knockout of *Ythdf1* in the D2 pathway showed significantly better performance (less inhibitory learning) during the probe phase (Figure 2.4E, S2.3C. 2.4E, unpaired t-test on day 15, $P=0.0398$), suggesting that inhibitory learning is mediated through the basal ganglia D2 pathway. Because YTHDF1 regulates protein synthesis rate, this result suggested that manipulating protein synthesis rate in the D2 pathway may prevent the formation of aberrant inhibitory learning under dopamine deficient conditions.

2.3.4 Computational Model supports preserved memory of normal learning in direct pathway after inhibitory learning

To recapitulate and understand how dopamine regulates the acquisition, impairment, and recovery of motor skill, we established a computational model based on the classical “cortico-basal ganglia-cortical loop” architecture (see Supplemental Information for the model description). In the model, the activity of motor cortex that controls the

rotarod task is modulated by a positive feedback loop via striatal D1 neurons (i.e. the direct pathway), as well as a negative feedback loop via D2 neurons (i.e. the indirect pathway) (Figure 2.5A). The core hypothesis underlying the model is the “cAMP-protein synthesis-memory consolidation” process (Figure 2.5B). We hypothesized that by regulating protein synthesis through dopamine receptor coupled cAMP pathway, consolidation of memory/plasticity is affected accordingly.[78,79] In the model, increased levels of dopamine activate both D1 and D2 dopamine receptors, which induces LTP and LTD in the equivalent connection weights of the positive and negative feedback pathways, respectively. Consequently, this facilitates the formation of memory in normal learning but diminishes inhibitory memory.[37] Further, the level of dopamine regulation is proposed to be proportional to the behavioral prediction error of the animal, which is anticorrelated to the task performance.[80]

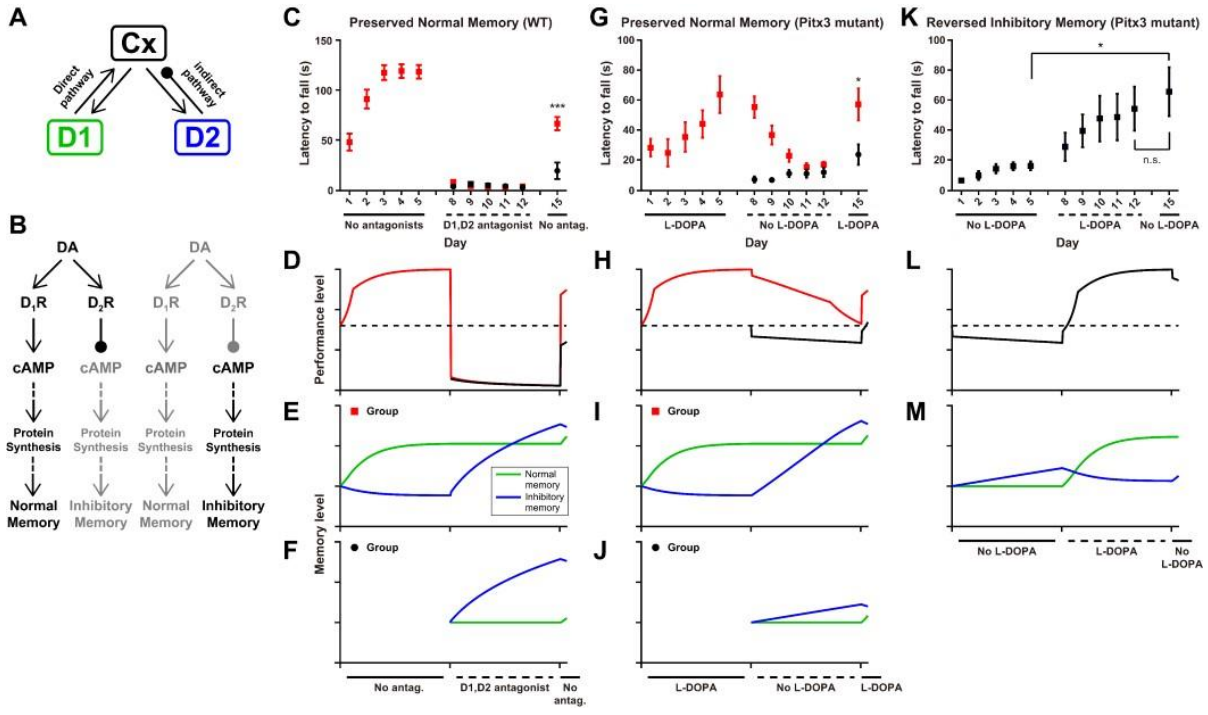

Fig 2.5. Modeling dopamine effects on mice rotarod performance under various experimental conditions.

Fig 2.5. cont.

(A) Schematic of the “cortico-basal ganglia-cortical loop” model containing direct and indirect feedback pathways. “Cx” reprsents the motor cortex.

(B) Schematic of the "cAMP-protein synthesis-memory consolidation" model of dopamine regulation on long-term plasticity of memories.

(C) Observed rotarod performance data in "normal learning – aberrant inhibitory learning – probe" (red) and “aberrant inhibitory learning – probe" (black) experimental design.

(D) Predicted rotarod performance by the model.

(E - F) The weights of memory of normal learning and aberrant inhibitory memory in the model.

(G − J) Similar to (C − F) but in Pitx3 mutant mice.

(K − M) Similar to (C − E) but in Pitx3 mutant mice using the “aberrant inhibitory learning - normal learning - probe" design.

We next tested if our computational model can recapitulate our behavior data. We found that the behavioral performance of WT mice in the experiments (Figure 2.5C) and model (Figure 2.5D) were well matched. Notably, during the aberrant inhibitory learning phase of the experiment, the application of dopamine antagonists blocks dopamine receptors, leading to an immediate drop of motor cortex activity and performance (Figure 2.5D). As training continues, the receptor blockade halts normal memory learning, but promotes the aberrant inhibitory memory learning (Figure 2.5E). During the probe phase where antagonists are removed, the normal memory is well preserved for the group with previous normal learning, but much weaker in the group without previous normal learning (Figure 2.5E vs 2.5F). This difference in the level of memory of normal learning explains the dramatic performance difference in the two groups right after drug

removal when the probe phase begins (Figure 2.5D). The recovery of memory of normal learning may not be 100% in WT or in Pitx3 mutant mice treated with L-DOPA (see below); it is affected by synaptic strength changes in both the direct and indirect pathways. We expect that many factors (e.g., dopamine receptor sensitivity, age, genetic background etc.) could contribute to the variation in the recovery strength.

Our model also recapitulates our behavior findings using Pitx3 mutant mice (Figure 2.5G, 2.5H). In the Pitx3 mutant mice, memory of normal learning is preserved while aberrant inhibitory learning is boosted during the “No L-DOPA” phase where the animals lack both endogenous and external dopamine (Figure 2.5I, 2.5J). One difference between the Pitx3 mutant mice and WT mice treated with antagonist is the smooth decay of motor cortical activity and performance over time during the aberrant inhibitory learning phase in Pitx3 mutant mice, rather than an instantaneous fall in WT mice treated with antagonist (Figure 2.5D vs 2.5H). One possible underlying mechanism is the adaptation of D1, D2 receptor activity to low dopamine level in the Pitx3 mutant mice (details in supplemental information).

Additionally, the model also captures the reversal of aberrant inhibitory memory in the ‘aberrant inhibitory learning-normal learning-probe’ schedule (Figure 2.5L, 2.5M). In the model, L-DOPA drives LTP and LTD of D1 and D2 pathways, respectively, leading to a boost of the memory of normal learning and decay of the aberrant inhibitory memory (Figure 2.5M, “L-DOPA” phase). The changes in the relative strength of memory of normal learning and aberrant inhibitory memory lead to improved performance level (Figure 2.5L, 2.5M), which would maintain even after the removal of L-DOPA before any

updates by additional learning (Figure 2.5L, the second “No drug” phase).

2.4 Discussion

Motor impairments in PD are often attributed to the lack of dopamine. However, our previously published studies[43,44,46] as well as the present data indicate that the impaired motor behavior is contributed largely by motor experience-dependent gradual deterioration of motor performance in the absence of dopamine or dopamine receptor activation, a mechanism that we refer to as aberrant inhibitory motor learning. Although the opposing consequences of normal motor learning and aberrant inhibitory learning are manifested in apparent motor performance, at the circuit level, memory of normal learning and aberrant inhibitory memory are stored in separate circuits, the former in the D1 (direct) pathway and the latter in the D2 (indirect) pathway. This is supported by our behavior results, fiber photometry recordings of GCaMP signals from dSPN and iSPN in the dorsal striatum, and genetic double dissociation of D1 pathway-dependent normal learning and D2 pathway-dependent aberrant inhibitory learning. It is also supported by a computational model based on activities of motor cortical neurons, D1 and D2 receptor-expressing neurons, and their interactions through the basal ganglia loops.

PD causes deteriorated motor control.[81,82] In animal models, our behavior results here showed that even though the impaired motor behavior was encoded into long term memory, the memory of normal learning learned under normal dopamine condition prior to the aberrant inhibitory learning is still preserved in the brain. These findings suggest

that reactivating preserved memory of normal learning could be therapeutic in PD. Indeed, in dopamine replacement therapy for PD, there are phenomena parallel to our findings in animal models. Long duration response is often observed in addition to the acute short duration response of the therapeutic effect.[39,83] The long duration response is a gradual buildup of the therapeutic effect through many days until it reaches the maximum strength, which is similar to the reversal of aberrant inhibitory learning by normal learning in our data (Figure 2.1F). On the other hand, the gradual decay of long duration response, which typically lasts many days after cessation of dopamine replacement therapy, is similar to the aberrant inhibitory learning process in our data (second phase in Figure 2.1D), i.e., the experience-dependent gradual deterioration of motor performance in the absence of dopamine signaling. Surprisingly, even after complete decay of long duration response, the first dose of L-DOPA or dopamine agonist in PD patients can often cause a complete rebound to the maximum therapeutic effect, without going through the gradual reversal of aberrant inhibitory learning by normal learning, similar to immediate reactivation of memory of normal learning in our data (Figure 2.1D).

Our fiber photometry studies give additional insights into the distinct roles played by D1 and D2 pathways in motor memory. A key observation is that high D1 pathway activities predict long rotarod trials whereas low D1 pathway activities predict short rotarod trials after aberrant inhibitory learning. This suggests that memory of normal learning stored in the D1 (direct) pathway remains largely intact and can be potentially reactivated, despite the progression of motor impairments in PD. Of note, due to the technical limitation of fiber photometry, we could not attain calcium dynamics at cellular

resolution. Future studies with more advanced imaging techniques will help understand the dynamics of normal and inhibitory memory engram during learning. Imaging technique with cellular resolution will also help us understand whether the changes we observe is due to somatic or non-somatic calcium activities, since a recent study showed that fiber photometry in striatum mostly reflect non-somatic changes.[84]

Both dopamine D1 and D2 receptors are coupled to Adenylyl cyclase 5 (AC5) and therefore the cAMP pathway. However, they have opposite effects on AC5 and protein kinase A (PKA) activity upstream of YTHDF1 and protein synthesis, with the D1 receptor activating while the D2 receptor inhibiting the cAMP pathway. It has been demonstrated that PKA activity in spiny projection neurons is dynamically influenced by dopamine differently in D1 versus D2 striatal neurons.[85,86] With increased dopamine, PKA is activated in D1 neurons. In contrast, PKA is activated in D2 neurons in dopamine-deficient states. Elevated cAMP and activated PKA can affect downstream signaling including the expression of immediate early genes, CREB, and new protein synthesis, all implicated in memory consolidation.[79,87,88] These mechanisms emphasize the essential role of elevated but not reduced cAMP that leads to new protein synthesis in memory consolidation, and may explain why the D1 pathway mediates normal motor learning and memory under normal dopamine whereas the D2 pathway mediates aberrant inhibitory motor learning and memory under dopamine deficiency. An alternative hypothesis to explain the distinct roles of the D1 versus D2 pathway in normal versus aberrant inhibitory learning/memory respectively is the receptor affinity hypothesis.[89] D1 receptors have low affinity for dopamine, therefore they are not

activated at the baseline condition, and they are more sensitive to increased dopamine release. In contrast, D2 receptors have high affinity for dopamine, therefore they are already activated at the baseline condition, and they are only sensitive to decreased dopamine release. This alternative hypothesis does not rely on the cAMP-new protein synthesis hypothesis. However, recent data challenges the D1 low affinity and D2 high affinity hypothesis.[90–94] Our computational model effectively corroborates our empirical results, lending further support to the cAMP-memory consolidation hypothesis. This computational approach also provides a powerful tool for predicting and understanding the complex dynamics of memory consolidation in the basal ganglia under varying conditions, and potentially guiding the development of targeted therapeutic strategies.

Our study highlights the integral role of protein synthesis in memory consolidation within the basal ganglia in addition to its well characterized role in the hippocampus.[95–97] The contrasting effects of *Ythdf1* knockout in the D1 versus D2 pathways suggest potential therapeutic targets for PD and other disorders. Most importantly, our result shows that conditional knocking out of *Ythdf1* in the D2 pathway did not affect normal learning process, but only mitigated the aberrant inhibitory learning, providing substantial therapeutic potential. Given that YTHDF1 targets the overall population of m^6A modified RNA, identifying the downstream targets of Ythdf1 for manipulating memory consolidation will be valuable for therapeutic development. By altering/modulating new protein synthesis pathways, it may be possible to enhance memory of normal learning and mitigate the consolidation of aberrant inhibitory memories. This approach could lead to novel treatments that focus not only on symptomatic relief but also on the

underlying synaptic neurobiological mechanisms of the disease which can potentially achieve long-lasting therapeutic effects.

Our findings also suggest compelling similarities between the aberrant inhibitory motor learning and the phenomenon of extinction learning. For example, in fear conditioning, current theories propose that extinction involves the formation of a new associative memory that inhibits the expression of the pre-existing memory, rather than erasing it.[67,98] This newly formed 'extinction memory' affects the manifestation of the antecedent memory trace. Similarly, we have demonstrated that aberrant inhibitory motor learning, induced by dopaminergic deficits and motor experience, does not erase pre-existing normal motor memories. Despite the similarities, there are also distinct features in our data: 1) there is clear anatomical segregation of pathways underlying memory of normal learning (D1 pathway) and aberrant inhibitory motor memory (D2 pathway). In extinction learning, no clear anatomical segregation has been reported; 2) aberrant inhibitory learning can be latent. When wild-type mice were treated with dopamine antagonists and trained on the rotarod, they apparently were not “learning” anything. However, their aberrant inhibitory learning was only revealed when they were trained again under no drug condition (Figure 2.1B). Even though latent extinction has been reported in the literature, it usually involves prevention of responses, and the mechanism is believed to be different from extinction learning.[99] In addition to the similarities to extinction learning, the concept of aberrant inhibitory learning can potentially be applied to other D2 pathway dependent learning under normal physiology conditions, such as reversal learning and discrimination.[23,28]

In conclusion, we have demonstrated that memory of normal learning is mostly stored in the D1 (direct) pathway whereas aberrant inhibitory motor memory is mostly stored in the D2 (indirect) pathway. The reactivation of either or both memories determines the apparent motor performance. These findings have important implications for novel therapeutic approaches in treating Parkinson's disease by reactivating preserved memory of normal learning, and in treating hyperkinetic movement disorders such as chorea or tics by erasing aberrant motor memories. The cAMP pathway and RNA binding proteins that facilitate new protein synthesis are important molecular targets to consider.

2.5 Method

2.5.1 Transgenic mice

2.5.1.1 Pitx3-mutant

Pitx3 (ak) mutant mice (Jackson Strain #:000942) exhibit an almost total loss of tyrosine hydroxylase-positive cells in the substantia nigra pars compacta, with a 90% decrease in dorsal striatal dopamine neuron at P0. The Pitx3 mutant mice are blind, yet this condition does not markedly influence their performance in the rotarod task used in the study.

2.5.1.2 Floxed *Ythdf1*, D1-Cre, A2a-Cre

Mice carrying a conditional removable *Ythdf1* allele ($Ythdf1^{f/f}$) were crossed to a D1-Cre

transgenic line (RRID: MMRRC-030989-UCD) or A2a-Cre transgenics line (RRID: MMRRC_036158-UCD) to selectively delete *Ythdf1* in D1 or D2 dopamine receptor expressing cells. All experiments were performed in both double transgenic mice (D1-Cre;Ythdf1$^{f/f}$, A2A-Cre;Ythdf1$^{f/f}$), and the respective control littermates.

2.5.2 Mouse Rotarod Behavior

Mice in the task are 8-12 weeks old unless otherwise stated. A computer-controlled rotarod apparatus (Rotamex-5, Columbus Instruments, Columbus, OH) with a rat rod (7cm diameter) was set to accelerate from 4 to 40 revolutions per minute over 300 seconds, and recorded time to fall. Mice received 5 consecutive trials per session, 1 session per day. Rest between trials was approximately 30 seconds.

2.5.3 Drug Administration

All drug injections were intraperitoneal at 0.01ml/gram of body weight. L-DOPA (3,4-dihydroxy-L-phenylalanine 25 mg/kg with 12.5mg/kg benserazide) was administered 1 hour prior to the start of each session. SCH 23390 at 0.1mg/kg and eticlopride at 0.16mg/kg were administered 30 minutes prior to experiments.

2.5.4 Stereotaxic Surgery

All surgical procedures were performed using mice aged 12-16 weeks under sterile conditions. Mice were anesthetized using 2% isoflurane and placed in a stereotaxic frame. Skull was exposed and bregma - lambda was identified, hole was drilled above dorsal striatum (AP +0.7, ML +2.25), a guide needle was lowered 2.7mm DV, 400nL of AAV virus (Addgene Catalog # 100838, AAV9.Syn.Flex.GCaMP6m.WPRE.SV40) was

delivered at a speed of 100nL/min, and allows for 7min to diffuse post injection before needle retraction. An optic cannula (MFC_400/430-0.66_5mm_MF1.25_FLT, Doric) was inserted into the injection site, 100μm above the viral delivery site. The cannula was then secured using surgical glue and dental cement.

2.5.5 Fiber photometry

TDT-Doric system was used for fiber photometry studies, TDT RZ5P for signal driving and demodulation. This system was adept at delivering light at wavelengths of 405 nm and 465 nm, while monitoring at 525 nm through a specialized Doric minicube (FMC5_IE(400- 410)_E(460-490)_F(500-540)_O(580-680)_S, Doric). The received light was processed by a femtowatt photodetector (Newport Model 2151), which then channeled the signals to the RZ5P. We used distinct modulation frequencies to monitor signals based on calcium dependence. The 465 nm excitation light was calcium-responsive and modulated at 331Hz, while the 405 nm, an isosbestic calcium-independent control, was modulated at 211 Hz using LEDs and LED driver (Doric). Mice were tethered to a patch cord (0.48NA, 400 μm core diameter, Doric) with freely rotary joint and gimbal holder (Doric) for maximum freedom during movement. The TDT Synapse software was employed to interact with the RZ5P system, facilitating data logging, event timestamping via TTL loggers, and LED control.

All data were analyzed in MATLAB with custom script, detailed code could be made available upon reasonable request. Briefly, first 5s recording was removed for opto-electro artifacts that might significantly affect the fitting parameters in the subsequent step. A smoothed 405nm signal was fitted to the 465nm signal using linear regression to

obtain fitting coefficients during a-3s baseline period before every rotarod trial. Using the coefficients, we calculated the fitted 405nm and calculated normalized ΔF/F for the calcium fluorescence.

2.5.6 Neuronal culture

Primary striatum neurons were cultured in 8-chambered coverglass systems (Cellvis C8-1.5H-N). Dissection was performed under a stereoscope utilized ice-cold 1x PBS, involving pia membrane removal and dorsal cortex dissection to expose the striatum. The dissected striatum tissues underwent enzymatic digestion with prewarmed Papain solution. After gentle chopping and incubation, the digested tissue was centrifuged, and cells were plated at a density of 0.04 million cells per well. Plating media transitioned to Neuromaintaining media after two hours. Medium maintenance involved replacing half the medium on day four and adding AraC to suppress gliogenesis. Subsequently, half the medium was regularly replaced every three days. Plating media included DMEM medium with 1% L-Glutamine, 1% penicillin–streptomycin, 0.8% Glucose, and 10% fetal bovine serum. Neuromaintaining media comprised Neurobasal medium with 1x B-27 supplement, 1x N2 supplement, 1% L-Glutamine, and 1% penicillin–streptomycin.

2.5.7 Click chemistry

Methionine-free DMEM was prepared by adding 4mM glutamine 0.4mM cysteine (thermo scientific #J60573.14, #J63745.14) into customized DMEM (thermo fisher #21013024) and stored at 4C. HPG Alexa Fluor™ 488 kit was purchased from Thermo Fisher (#C10428). Cultured cells were gently washed with PBS and changed into

methionine-free DMEM for 1-hour to decrease the intracellular methionine concentration. 5 μg/ml CHX and 10 μM Forskolin were added 10 minutes before adding HPG. Cells were added with a final concentration of 100 μM, HPG and incubated for 2 hours. Cells are washed with PBS and followed up with HPG labeling process described in protocol from thermo fisher. Cells are washed with PBS and incubated with MAP2 antibody (Sigma-Aldrich, Cat# M4403) for 2 hours at room temperature before the DNA staining step.

2.5.8 Quantification and statistical analysis

Data are reported as mean ± SEM, and n represents the number of mice used per experiment unless otherwise stated. Statistical analyses were conducted in Graphpad. Statistical significance was assessed using a student's t test or repeated-measures ANOVA for experiments that tracked behavior over time or repeated training, as well as fiber photometry experiments that compare different trials from different mouse groups. For significant findings after ANOVA, post-hoc Tukey's HSD tests were used to identify specific group differences. The level of significance was set at $p < 0.05$.

2.5.9 Computational model

Details are available online[100].

2.6 Author Contributions

K.W. and X.Z. conceived the project and experiments. P.Y., K.W., X.Z. and B.D. conceived the computational model. K.W. and Z.S. performed most of the experiments

with help from L.M., K.W., V.Y., N.W. and J.B.. S.S. and D.M. helped with fiber photometry experimental design and data analysis. P.Y. built the computational model. K.W., P.Y. and X.Z. wrote the first draft of the manuscript while all authors contributed to the writing.

2.7 Acknowledgements

We thank Benjamin Wang, Nabilah Sammudin, Nicholas LoRocco and Wenqin Fu for helpful discussions and comments on the manuscript. This work was supported by R01DA043361 (X.Z.), R01NS095374 (X.Z. and D.M.), Simons Foundation Collaboration on the Global Brain (B.D.), NIH 1U19NS107613-01 (B.D.), R01EB026953 (B.D.), and R01EY034723 (B.D.). Shared equipment grants from the University of Chicago Neuroscience Institute supported the shared fiber photometry, AAV injection, and histology facilities.

2.8 Declaration of Interests

The authors declare no competing interests.

2.9 Supplementary Figures

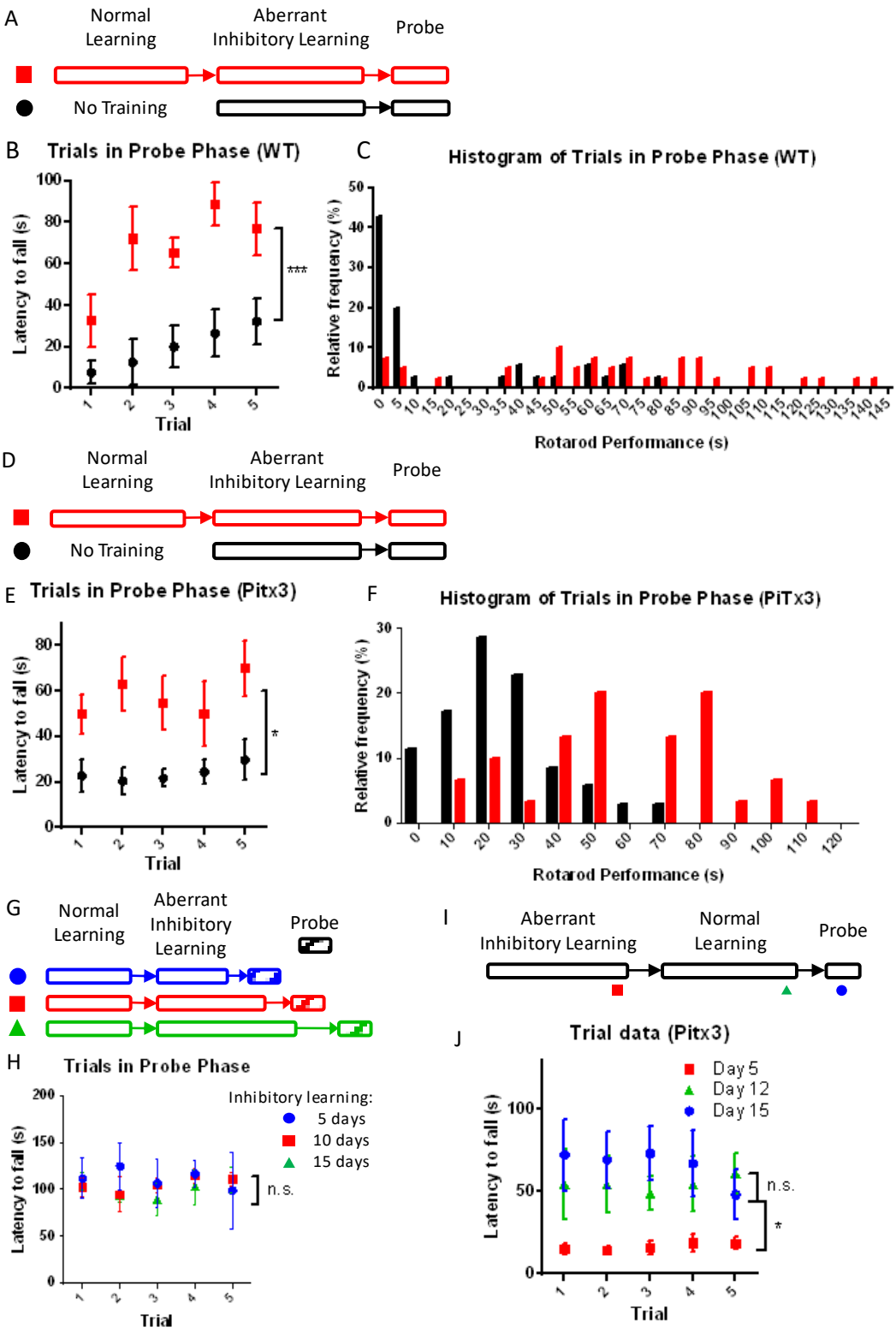

Fig S2.1. Individual trial data for different rotarod experiments.
(A, D, G, I) Behavior paradigms used in each experiment and different phases of normal

Fig S2.1. cont.
learning and aberrant inhibitory learning.
(A-C) Preserved memory of normal learning after aberrant inhibitory learning in WT mice.
(B) Individual trial data from figure 1C on day 15, two-way ANOVA, group effect $F(1, 13) = 20.35$, $p = 0.0006$; group x time interaction, $F(4, 52) = 1.239$, $p = 0.3058$.
(C) Histogram of rotarod performance on probe phase.
(D-F) Preserved memory of normal learning after aberrant inhibitory learning in Pitx3 mutant mice.
(E) Individual trial data from day 15 in figure 1D, two-way ANOVA, group effect $F(1, 11) = 8.317$, $p = 0.0149$, group x time interaction, $F(4, 44) = 1.587$, $p = 0.1945$.
(F) Histogram of rotarod performance on probe phase.
(G-H) Preserved memory of normal learning after various days of aberrant inhibitory learning in Pitx3 mutant mice.
(H) Individual trial data from probe phase after various days of aberrant inhibitory learning from figure 1E. Two-way ANOVA between three groups with different length of inhibitory learning, group effect $F(2, 17) = 0.255$, $p = 0.778$; group x time interaction $F(8, 68) = 0.372$, $p = 0.932$.
(I-J) Inhibitory memory was reversed by normal learning experience in Pitx3 mutant.
(I) Experimental design with red, green and blue symbols showing different time points for comparison.
(J) Individual trial data on day 5, 12, 15 from figure 1F. Two-way ANOVA with repeated measures between day 5 and day15, day effect $F(1, 7) = 11.80$, $p = 0.022$. Two-way ANOVA with repeated measures between day 12 and day15, day effect $F(1, 7) = 3.650$, $p = 0.195$. P values are adjusted using Bonferroni correction.
All data represents mean ± SEM. *, $p<0.05$; **, $p<0.01$; ***, $p<0.001$. n.s., not significant.

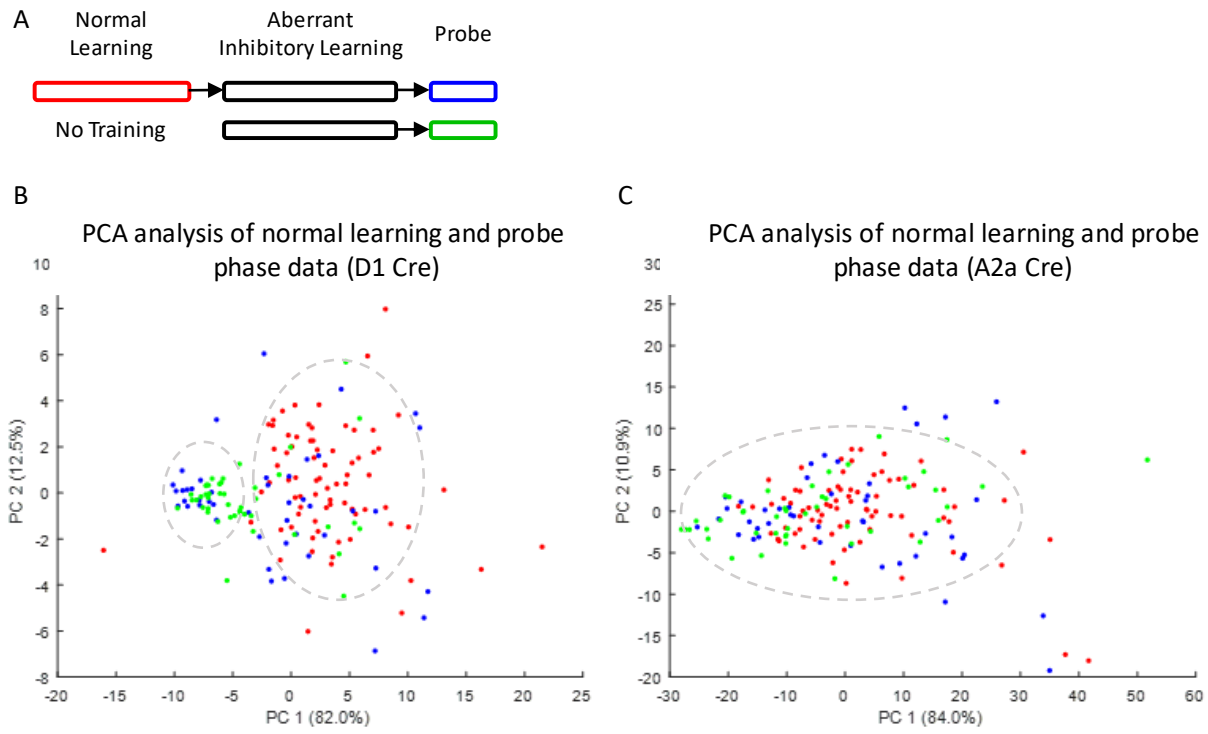

Fig S2.2. PCA analysis of fiber photometry signal
(A) Behavior experiment design and color code for data points from different phases. The red, blue and green section shows where the data were collected in fig S2B-C.
(B) Plotting dSPNs fiber photometry data using principal component 1 and 2 from PCA analysis. Red, normal learning data; blue, probe phase data from the group trained in normal learning phase; green, probe data from the group not trained in normal learning phase.
(C) Plotting iSPNs fiber photometry data using principal component 1 and 2 from PCA analysis. Color codes are the same as figure S2A.

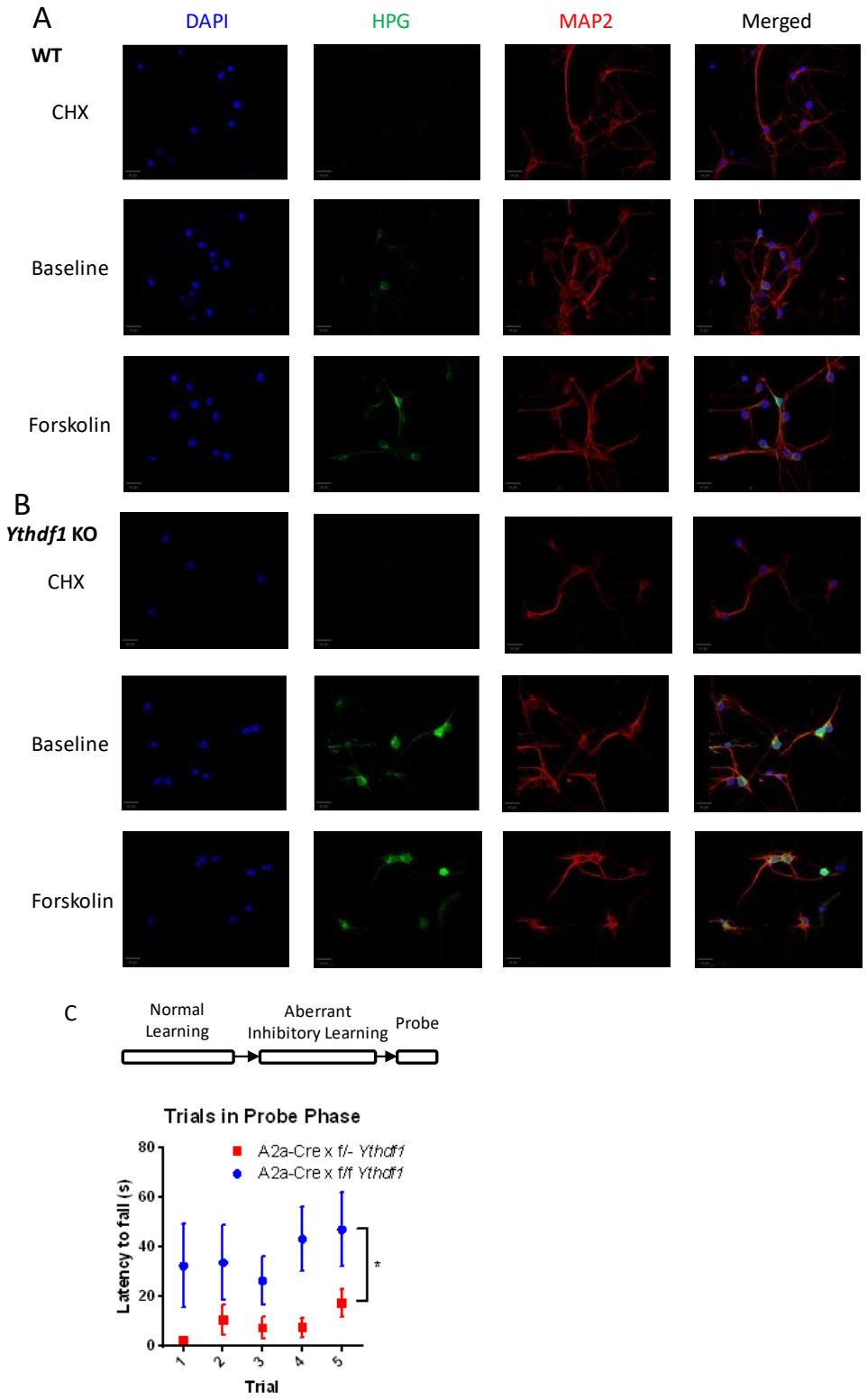

Fig S2.3. Measuring new protein synthesis in *Ythdf1* KO using Click chemistry. (A) Newly synthesized protein in WT control. Left-right: DAPI, HPG signal, MAP2, merged; top-bottom: CHX treated, baseline and forskolin treated group. Scale bar,

Fig S2.3. cont.
20um.
(B) Newly synthesized protein in *ythdf1* KO. Left-right: DAPI, HPG signal, MAP2, merged; top-bottom: CHX treated, baseline and forskolin treated group. Scale bar, 20um.
(C) Individual trials of rotarod performance from probe phase (day 15 in Figure 4E). Two-way ANOVA, Group effect, $F(1, 9) = 5.764$, $p=0.0398$. Group x time interaction $F(4, 36) = 0.5931$, $p=0.6698$. n(A2a Cre x f/f *Ythdf1*) = 5. n(A2a Cre x f/- *Ythdf1*) = 6.

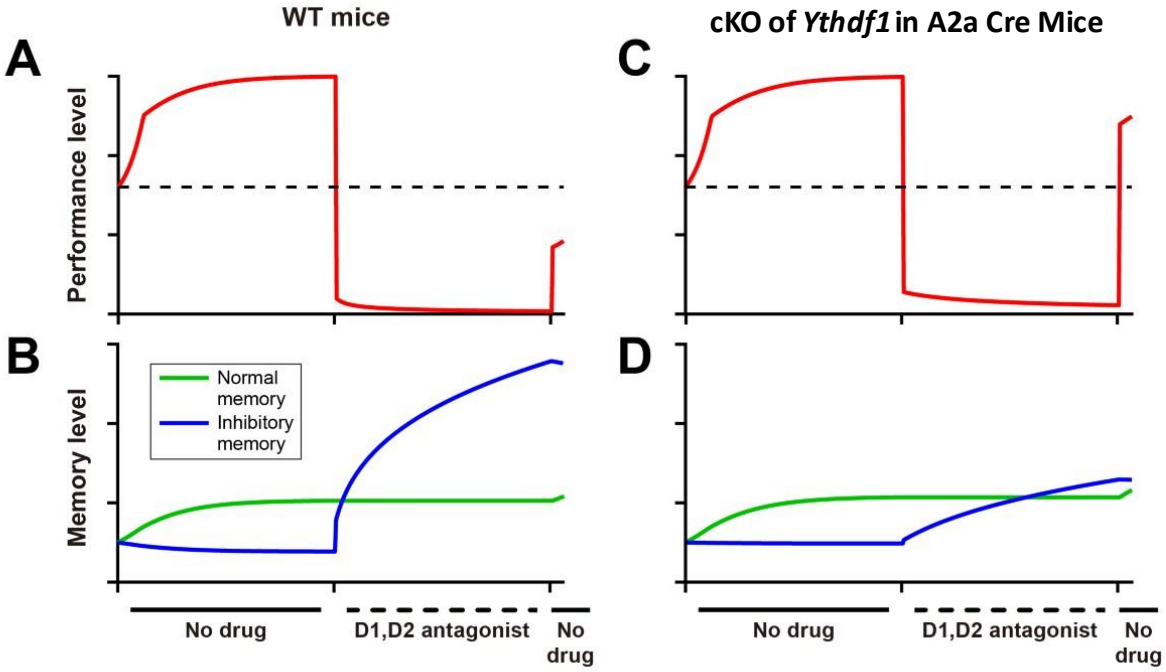

Fig S2.4. Computational model describing rotarod motor learning and performance in mice with conditional *Ythdf1* gene deletion in A2a Cre mice.
(A) Behavior of WT mice predicted by the model in a "normal learning - aberrant inhibitory learning - probe" design.
(B) The weights of memory of normal learning and aberrant inhibitory memory in the model.
(C − D) Similar as (A − B) but in mice with A2a-Cre mediated conditional *Ythdf1* gene deletion where the inhibitory learning rate becomes 10% of the normal rate.

CHAPTER 3 NEURAL PATHWAYS AND MOLECULAR MECHANISMS IN NORMAL AND ABERRANT INHIBITORY LEARNING

3.1 Abstract

Dopamine loss or blockade causes aberrant inhibitory learning in Parkinson's disease in addition to the acute motor inhibition. While we showed that memory of normal learning can be preserved after aberrant inhibitory learning, the neuronal population for storing normal and aberrant inhibitory memory is not yet discovered. We here used cFos as a neuronal activity marker and identified the M2 cortex as a region enriched in neuronal population underlying normal and aberrant inhibitory. Furthermore, how aberrant inhibitory learning is consolidated through the intracellular pathway is not fully understood. We utilized a chemogenetic approach to manipulate cAMP signaling in various conditions to investigate intracellular signaling underlying normal and aberrant inhibitory learning. In the end, we took advantage of our findings and explored strategies to rescue or reverse aberrant inhibitory learning underlying Parkinson's disease.

3.2 Introduction

In Chapter 3, we extend our investigation into the complex interaction between aberrant inhibitory motor memory and normal motor learning. One key question is: where are normal and aberrant inhibitory memories located in the brain? To address this, we took advantage of immediate early genes, such as cFos, as markers of neuronal activity.

Their expression patterns may not only label the neuronal population underlying both types of learning but also unveil the specific neuronal circuits implicated in PD.

Our computational model (chapter 2) focused on the ‘cAMP-CREB-memory consolidation’ process in consolidating both normal and aberrant inhibitory memory. In pursuit of understanding and potentially regulating the aberrant inhibitory learning process, we take advantage of the Designer Receptors Exclusively Activated by Designer Drugs (DREADDs) technology[101]. This chemogenetic method allows for the manipulation of cAMP levels and neuronal activity in selective pathways. By employing engineered receptors that can be selectively activated by synthetic ligands, DREADDs facilitate the targeted investigation of neuronal circuits and their roles in various behaviors and pathologies, including Parkinson's disease.

In addition to cAMP pathways, the β-arrestin pathway, distinct from traditional G protein-mediated signaling, plays an important role in cellular responses to external signals[102]. Within the context of PD, the β-arrestin pathway emerges as a critical modulator of dopamine receptor function and the subsequent cascade of signaling events, which are vital for motor control and the learning process. We aim to investigate how β-arrestin is involved in aberrant inhibitory learning mediated by dopamine loss.

Through exploring these mechanisms, this chapter aims to investigate how the neuronal population and intracellular signaling are involved in aberrant and normal motor learning, and how targeted manipulation of these pathways could provide novel

therapeutic targets to treat the motor decline associated with neurodegenerative diseases.

3.3 Results

3.3.1 Exploring cFos Expression in Normal and Inhibitory Learning (WT)

To study the neuronal population involved in normal and aberrant inhibitory learning, we use cFos as a neuronal activity marker and examine their expression in mice under different training experience[103]. Mice are divided into three groups (Figure 3.1A): the 'normal learning' group are trained for one week on rotarod; the 'aberrant inhibitory learning' group are trained for one week with the treatment of dopamine D1 and D2 antagonists cocktail; the 'home cage' group are kept in the mouse cage as negative control. Normal and inhibitory learning groups are given a probe training session in the second week. Following a probe training session in the second week, we collected brain sections from all groups to analyze cFos expression in key areas associated with motor learning: the dorsal medial striatum (DMS), M1, and M2 motor cortex (Figure 3.1C). As expected, the normal learning group showed a significant better performance than the inhibitory learning group during the probe phase (Figure 3.1B, Two-way ANOVA, group effect, $F(1, 14) = 37.76$, $p < 0.0001$; group x time interaction $F(4, 56) = 0.2122$, $p = 0.9306$).

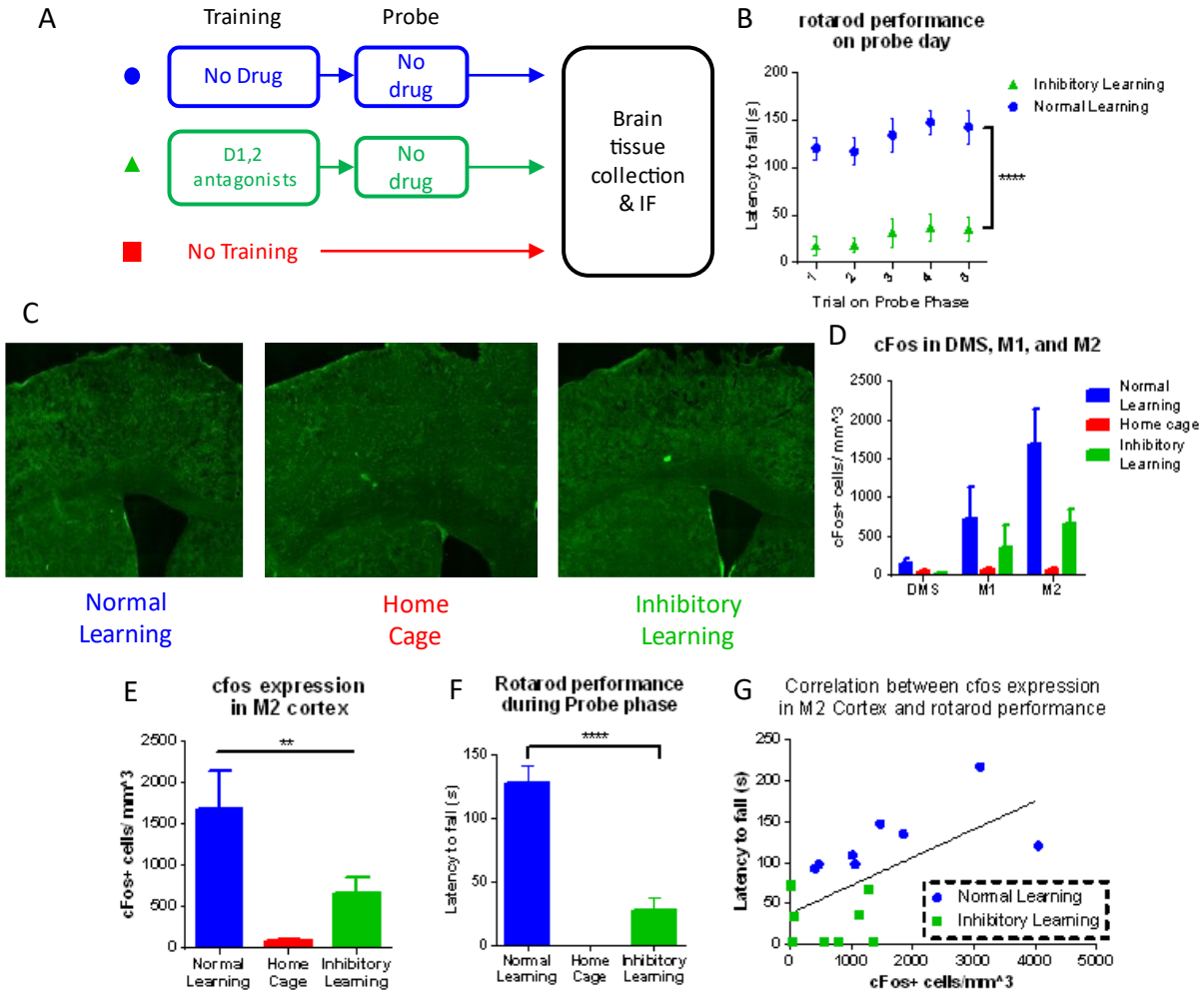

Fig 3.1. Neuronal activity in normal and aberrant inhibitory motor learning (WT mice)

(A) Experimental designs for normal motor learning (blue) and aberrant inhibitory motor learning (green) and home cage control group. Mice were trained according to the protocol and brain tissues were collected 1 hour after training for immunostaining.

(B) Normal learning group performed significantly better than the aberrant inhibitory learning group during the probe phase. Two-way ANOVA, group effect, $F(1, 14) = 37.76$, $p < 0.0001$; group x time interaction $F(4, 56) = 0.2122$, $p = 0.9306$, $n = 8$ for each group.

(C) Representative images of cFos immunostaining in the dorsal str, M1, M2 areas in the three groups of mice.

(D) cFos expression level in the dorsal str, M1, M2 areas in the three groups of mice.

(E) cFos expression level in M2 cortex in the three groups of mice. One way ANOVA, group effect, $F(2,21) = 8.02$, $p = 0.0026$, $n = 8$ for each group.

Fig 3.1. cont.
(F) Mean rotarod performance on the test day for the three groups of mice. unpaired T-test between normal learning group and aberrant inhibitory learning group, $p < 0.0001$, $n = 8$ for each group.
(G) Linear correlation between cFos expression level and rotarod performance using the normal learning and inhibitory learning groups. Each dot represents one mice. Fitting equation $Y = 0.034*X + 37.3$, $R^2 = 0.37$.
All data represents mean ± SEM. *, $p<0.05$; **, $p<0.01$; ***, $p<0.001$; ****, $p<0.0001$. n.s., not significant.

As a negative control, cFos expression was minimal in the home cage control group across all examined brain regions, aligning with expectations for non-trained mice (Figure 3.1D). A comparative analysis of cFos expression in the DMS, M1, and M2 across the experimental and control groups revealed notably higher cFos levels in the M2 motor cortex than in the M1 and DMS regions (Figure 3.1D). Although cFos expression in the DMS remained low across all groups, a slight increase was observed in the normal learning group. Given these expression patterns, we focused on the M2 motor cortex in the following analysis, where the differential expression of cFos was most evident.

We observed a significant difference in M2 cFos expression among the normal learning, aberrant inhibitory learning, and home cage groups (Figure 3.1E, One way ANOVA, group effect, $F(2,21) = 8.02$, $p = 0.0026$), with the normal learning group exhibiting elevated cFos expression compared to the aberrant inhibitory learning group. This difference aligns with their respective motor performances on the rotarod, where the normal learning group performed better than the aberrant learning group (Figure 3.1F, unpaired T-test, $p < 0.0001$), suggesting that cFos expression is a potential indicator of

performance duration. A correlation analysis further supported this, demonstrating a positive relationship between rotarod performance and cFos expression levels (Figure 3.1G, $Y = 0.034*X + 37.3$, $R^2 = 0.37$). This result suggests that M2 cFos expression reflects the extent of motor activity, with greater activity correlating with higher cFos expression. Interestingly, a similar pattern was observed in the M1 cortex, though with a less overall cFos expression level (Figure 3.1D).

3.3.2 Exploring cFos Expression in Normal and Inhibitory Learning (Pitx3 mutant)

We next assessed neuronal activity in Pitx3 mutant mice using a similar strategy. These mice were divided into three groups (Figure 3.2A): a 'home cage' control group, which remained untrained; a 'normal learning' group, which received L-DOPA injections and were trained on rotarod for one week; and an 'aberrant inhibitory learning' group, which underwent rotarod training without L-DOPA for a week to induce inhibitory learning. Following the training, both the normal and aberrant inhibitory learning groups underwent a one-day rotarod session without L-DOPA during the probe phase to evaluate the recall of motor memory. Subsequent brain tissue collection from all mice allowed for cFos immunostaining analysis. Consistent with our earlier findings, the normal learning group performed better than the aberrant inhibitory learning group in the probe phase (Figure 3.2B, Two-way ANOVA, group effect, $F(1, 9) = 9.55$, $p = 0.013$; group x time interaction $F(4, 36) = 1.027$, $p = 0.407$).

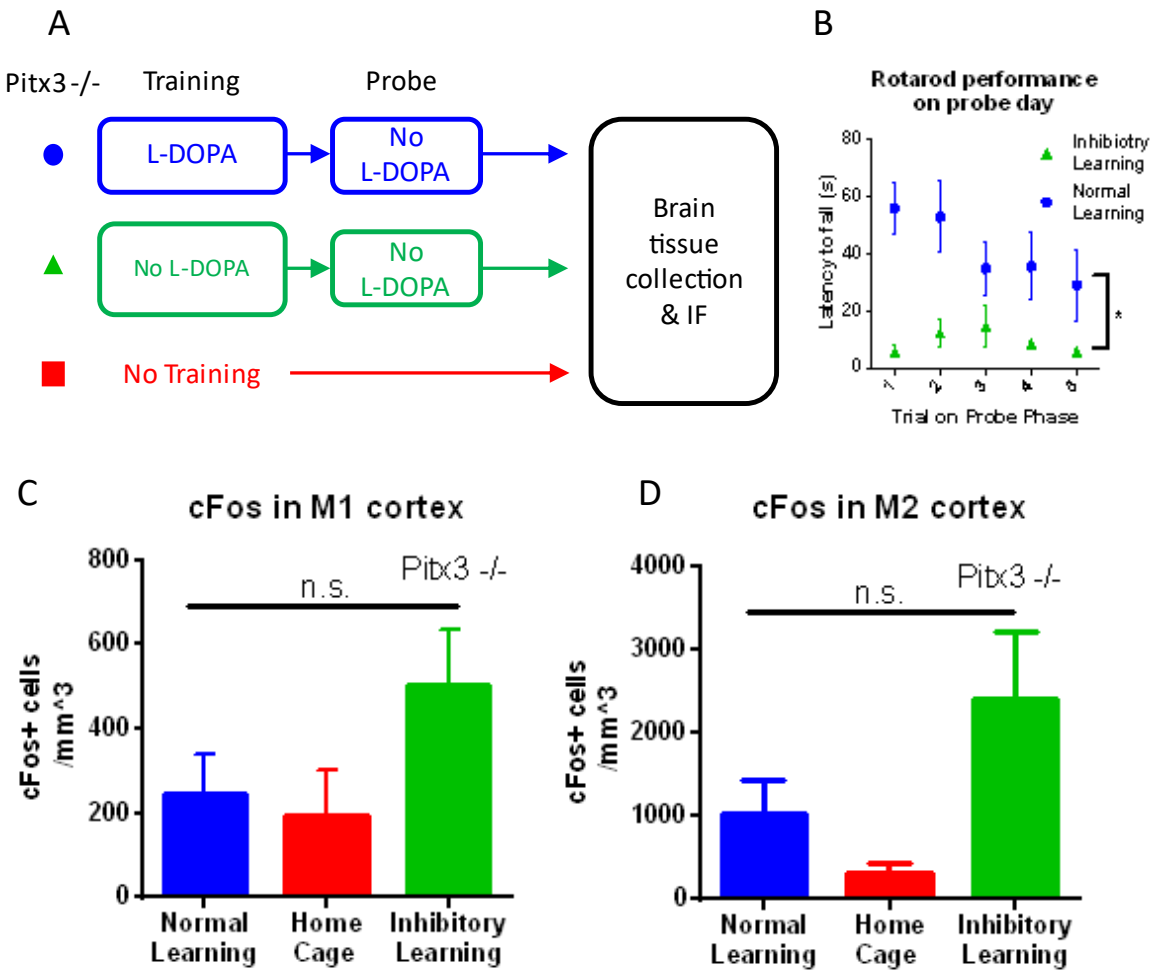

Fig 3.2. Neuronal activity in normal and aberrant inhibitory motor learning (Pitx3 -/- mice)

(A) Experimental designs for normal motor learning (blue) and aberrant inhibitory motor learning (green) and home cage control group (red) using Pitx3 (-/-) mice. Mice were trained according to the protocol and brain tissues were collected 1 hour after training for immunostaining.

(B) Normal learning group performed significantly better than the aberrant inhibitory learning group during the probe phase. Two-way ANOVA, group effect, $F(1, 9) = 9.55$, $p = 0.013$; group x time interaction $F(4, 36) = 1.027$, $p = 0.407$; n (normal learning) = 8, n(inhibitory learning) = 4.

(C) cFos expression level in M1 cortex in the three groups of mice. One way ANOVA, group effect, $F(2,17) = 1.975$, $p = 0.1693$, n = 8 for normal and inhibitory learning groups, n = 4 for home cage group.

(D) cFos expression level in M2 cortex in the three groups of mice. One way ANOVA,

Fig 3.2. cont.
group effect, F(2,17) = 2.547, p = 0.1078, n = 8 for normal and inhibitory learning groups, n = 4 for home cage group.
All data represents mean ± SEM. *, p<0.05. n.s., not significant.

Similar to observations in WT mice, cFos expression within the striatum of Pitx3 mutant mice remained notably low. Thus, we focus towards the M1 and M2 motor cortex where cFos expression was predominantly observed. In the M1 motor cortex, a marginal increase in cFos expression was observed in the inhibitory learning group when compared to both the home cage and normal learning groups. However, this trend did not reach statistical significance (Figure 3.2C, One way ANOVA, group effect, F(2,17) = 1.975, p = 0.1693), indicating that the variations in cFos levels might represent baseline neural activity rather than being directly attributable to rotarod training. This result indicates that, in the M1 cortex, cFos expression levels between the normal motor learning and home cage groups are similar, suggesting cFos is representing a baseline activity rather than a specific response to motor training.

Conversely, the M2 motor cortex presented a more pronounced difference in cFos expression among the three groups, with the home cage mice displaying the lowest level of cFos. Notably, the inhibitory learning group exhibited a trend towards increased cFos expression relative to the normal learning group, although this did not reach statistical significance (Figure 3.2D, One way ANOVA, group effect, F(2,17) = 2.547, p = 0.1078). Given that the inhibitory learning group experienced substantially less rotarod activity compared to their normal learning counterparts (Figure 3.2B), the elevated cFos expression in the M2 cortex for the inhibitory group intriguingly suggests its potential

role in encoding inhibitory learning memories in Pitx3 mutant mice. Further research is needed to understand the specific contributions of the M2 cortex to the aberrant motor learning process.

3.3.3 Investigating the cAMP pathway via DREADDs in normal and inhibitory learning

After studying the neuronal population of normal and aberrant inhibitory learning, we next investigate how intracellular signaling contribute to these learning phenomenon. In the previous chapter, both our computational models and experimental findings highlighted the crucial role of the dopamine receptor-mediated 'cAMP-CREB-protein synthesis' pathway in facilitating both normal and inhibitory learning processes. To further investigate this, we utilized a variety of chemogenetic strategies targeting the D1 and D2 pathways, aiming to assess their impact on these distinct learning behaviors.

We first investigated whether activating Gαs signaling in the D2 pathway is sufficient to induce aberrant inhibitory learning. In the open field test, administering 0.01mg/kg of DCZ to A2a-Gαs DREADDs mice resulted in a marked reduction of motor activity (Figure 3.3B, Two-way ANOVA, group effect, $F(1, 12) = 4.91$, $p = 0.047$; group x time interaction $F(10, 120) = 0.938$, $p = 0.501$), in contrast to saline-treated mice, which showed no significant behavioral changes when compared to controls (Figure 3.3A). This finding aligns with earlier reports highlighting the selective modulation of cAMP production by Gαs DREADD in striatopallidal neurons[104]. We next treated A2a-Gαs

DREADDs mice with 0.01 mg/kg DCZ and trained them on rotarod. However, during one week of DCZ treatment and also the probe phase in the second week, we found no difference between the control group and the A2a-Gαs DREADDs mice (Figure 3.3C, Two-way ANOVA, group effect, $F(1, 12) = 0.438$, $p = 0.52$; group x time interaction $F(34, 408) = 0.888$, $p = 0.652$). To avoid the possibility that the lack of behavior phenotype is caused by low dose of DCZ, we even tested a dose 10 time higher (0.1mg/kg DCZ), which resulted in similar observation (Figure 3.3D, Two-way ANOVA, group effect, $F(1, 11) = 0.153$, $p = 0.703$; group x time interaction $F(34, 374) = 1.145$, $p = 0.269$). These results indicate that Gαs signaling activation within iSPNs alone is not sufficient to impair motor function in the rotarod task, suggesting the involvement of additional factors or pathways.

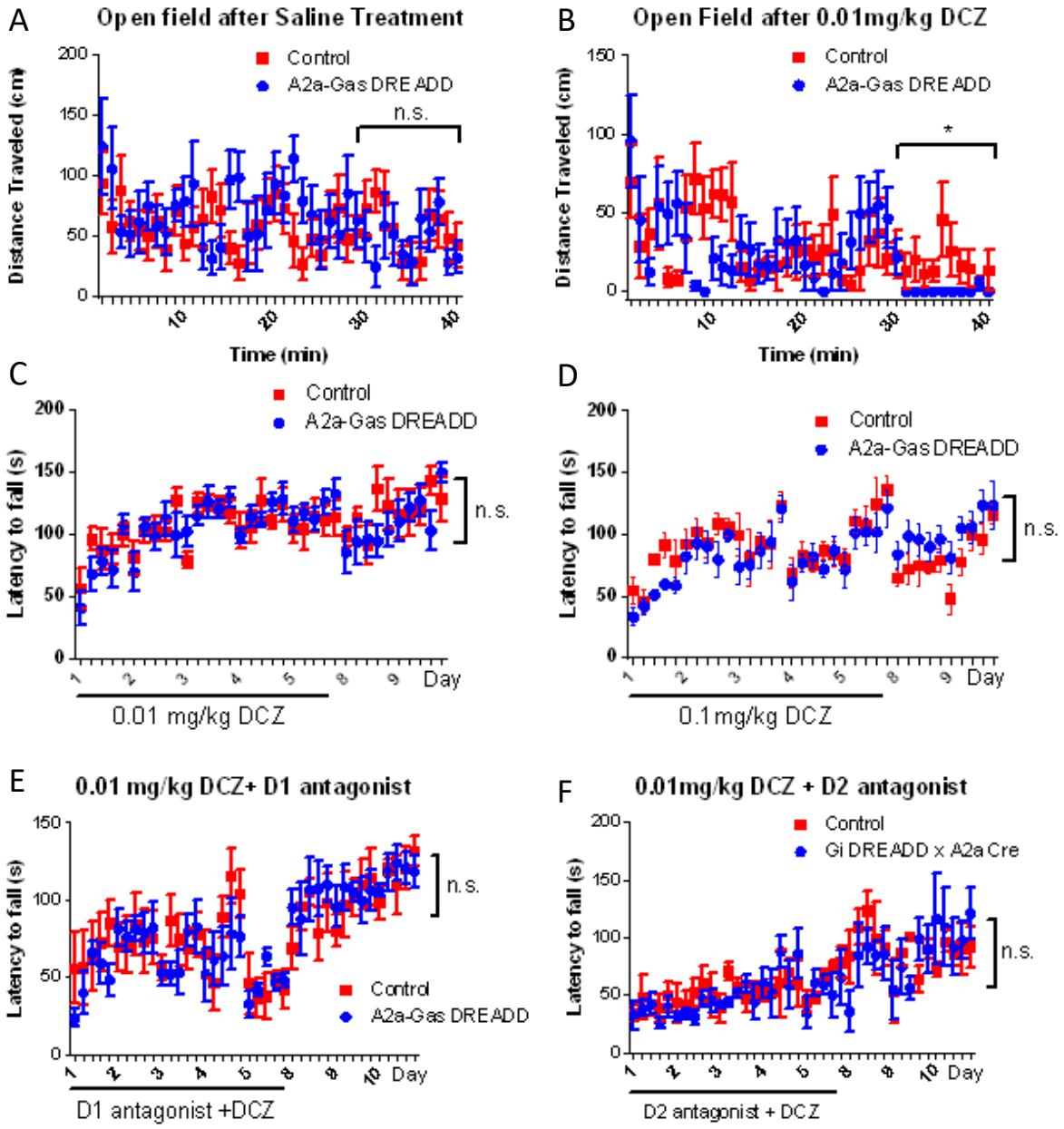

Fig 3.3. Chemogenetic studies on normal and aberrant inhibitory learning
(A) Open field experiment immediate after saline treatment for A2a-Gas DREADDs and control mice. Two-way ANOVA for 30-40 min, group effect, $F(1, 12) = 0.267$, $p = 0.615$; group x time interaction $F(10, 120) = 1.161$, $p = 0.324$; $n = 7$ for each group.
(B) Open field experiment immediate after 0.01 mg/kg DCZ treatment for A2a-Gas DREADDs and control mice. Two-way ANOVA for 30-40 min, group effect, $F(1, 12) = 4.91$, $p = 0.047$; group x time interaction $F(10, 120) = 0.938$, $p = 0.501$; $n = 7$ for each

Fig 3.3. cont.
group.
(C) Rotarod performance 35min after 0.01 mg/kg DCZ treatment for A2a-Gas DREADDs and control mice. Mice were treated with DCZ for 1-5 days. Two-way ANOVA, group effect, F (1, 12) = 0.438, p = 0.52; group x time interaction F (34, 408) = 0.888, p = 0.652; n = 7 for each group.
(D) Rotarod performance 35min after 0.1 mg/kg DCZ treatment for A2a-Gas DREADDs and control mice. Mice were treated with DCZ for 1-5 days. Two-way ANOVA, group effect, F (1, 11) = 0.153, p = 0.703; group x time interaction F (34, 374) = 1.145, p = 0.269; n = 7 for each group.
(E) Rotarod performance 35min after 0.1 mg/kg DCZ and 0.1 mg/kg SCH 23390 treatment for A2a-Gas DREADDs and control mice. Mice were treated with DCZ and SCH 23390 for 1-5 days. Two-way ANOVA, group effect, F (1, 10) = 0.065, p = 0.80; group x time interaction F (39, 390) = 0.85, p = 0.71; n = 6 for each group.
(F) Rotarod performance 35min after 0.01 mg/kg DCZ and 0.16 mg/kg Eticlopride treatment for A2a-Cre x Gi DREADDs and control mice. Mice were treated with DCZ and Eticlopride for 1-5 days. Two-way ANOVA, group effect, F (1, 5) = 0.08, p = 0.79; group x time interaction F (39, 195) = 0.96, p = 0.55; n (A2a-Cre x Gi DREADDs) = 4, n (control) = 3.
All data represents mean ± SEM. *, p<0.05. n.s., not significant.

We next test if activating Gαs signaling in the D2 pathway is sufficient to consolidate a impaired behavior into long-term memory. Our previous findings showed that impaired behavior induced by D1 antagonists was temporary and failed to consolidate into long-term memory[43]. We hypothesized that this temporary impairment might be due to reduced cAMP levels in dSPNs, thereby preventing the memory consolidation process. To examine whether artificially elevating cAMP levels in iSPNs (the indirect pathway) could lead to the consolidation of such impaired behavior into long-term memory, we administered D1 antagonists and 0.01 mg/kg DCZ to both A2a-Gαs DREADDs mice and a control group during a week of rotarod training. Throughout this phase, both groups exhibited comparable levels of impaired behavior (Figure 3.3E). Subsequent testing on the rotarod without drug treatment aimed to determine if increased cAMP in iSPNs could solidify this behavior into lasting memory. Contrary to our expectations, no

significant performance difference was observed between the two groups (Figure 3.3E, Two-way ANOVA, group effect, $F(1, 10) = 0.065$, $p = 0.80$; group x time interaction $F(39, 390) = 0.85$, $p = 0.71$), suggesting that merely boosting cAMP levels in iSPNs, even amidst impaired behavior, does not facilitate the conversion of this behavior into persistent memory in the indirect pathway. This outcome showed the complexity of the memory consolidation process, suggesting that the impaired behavior induced by D1 antagonists—primarily affecting the D1 pathway—cannot be effectively consolidated into long-term memory through manipulations of the D2 pathway via increasing cAMP signaling pathway.

After testing the sufficiency of cAMP pathway in aberrant inhibitory learning, we want to address whether change in cAMP level is required for aberrant inhibitory learning. Our previous observations showed caffeine treatment can mitigate aberrant inhibitory learning (unpublished), and given that one of the main function of caffeine is an A2a antagonist reducing cAMP levels in iSPNs, we proceeded to test whether diminishing cAMP via Gi DREADDs in the indirect pathway could similarly prevent the consolidation of aberrant inhibitory learning. To explore this, we used mice engineered to express Gi DREADDs specifically in iSPNs— by breeding Cre-dependent Gi DREADDs mice with A2a-Cre mice. These mice were then treated with a D2 antagonist to trigger aberrant inhibitory learning and DCZ to lower cAMP levels in iSPNs, before being trained on the rotarod for a week. A subsequent rotarod probe phase post-training, without any pharmacological intervention, also failed to demonstrate significant differences between the groups (Figure 3.3F, Two-way ANOVA, group effect, $F(1, 5) = 0.08$, $p = 0.79$; group

x time interaction F(39, 195) = 0.96, p = 0.55). This finding contrasts with our caffeine results, suggesting that a simple reduction in cAMP within iSPNs may not suffice to prevent the consolidation of aberrant learning. This discrepancy underscores the need for further research to identify the optimal conditions—potentially through modifications in the training protocol or adjustments in DCZ dosage—that could effectively mitigate aberrant inhibitory learning by modulating cAMP levels in iSPNs.

3.3.4 β-arrestin is not required for inhibitory learning

Our findings suggest that beyond cAMP signaling, additional pathways may contribute to aberrant inhibitory learning. One possibility is the non-canonical β-arrestin pathway. Prior studies have indicated that β-arrestin's engagement with the dopamine D2 receptor influences locomotion without affecting incentive motivation[105]. To test whether β-arrestin signaling plays a role in aberrant inhibitory learning, we treated β-arrestin KO mice with a cocktail of D1 and D2 antagonists and trained them on rotarod training for a week, followed by a recovery phase without drug treatment. The performance during the training and recovery phases showed minimal performance disparities between the β-arrestin KO and the control group (Figure 3.4A, Two-way ANOVA, group effect, F (1, 13) = 0.08, p = 0.78; group x time interaction F(39, 507) = 0.363, p = 0.99). This result suggests that β-arrestin does not play a crucial role in the development of aberrant inhibitory learning.

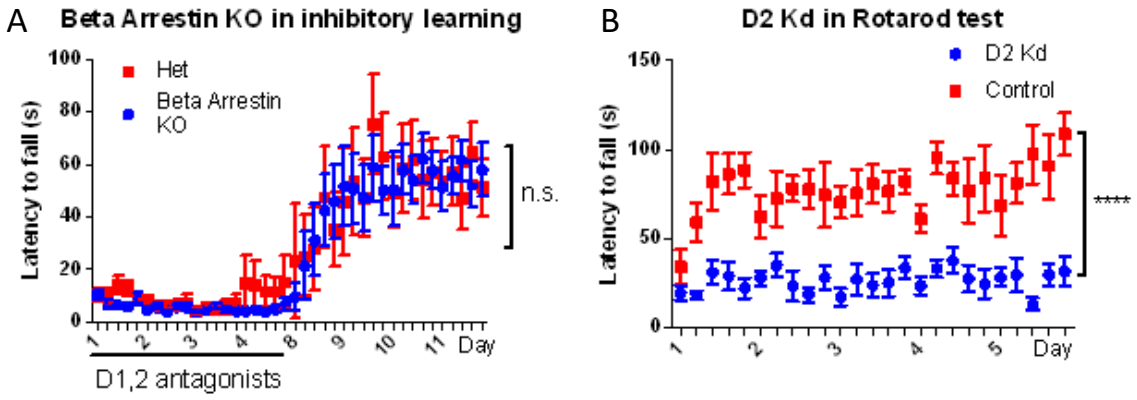

Fig 3.4. Signaling pathways in normal and aberrant inhibitory learning
(A) Rotarod performance 30min after 0.1 mg/kg SCH 23390 and 0.16 mg/kg Eticlopride treatment for β-arrestin KO and control mice. Mice were treated with dopamine antagonists cocktail for 1-4 days. Two-way ANOVA, group effect, $F(1, 13) = 0.08$, $p = 0.78$; group x time interaction $F(39, 507) = 0.363$, $p = 0.99$; n(β-arrestin) = 8, n(control) = 7.
(B) Rotarod performance for D2 Kd and control mice. Two-way ANOVA, group effect, $F(1, 10) = 58.86$, $p < 0.0001$; group x time interaction $F(24, 240) = 1.124$, $p = 0.32$; n = 6 for each group.
All data represents mean ± SEM. ****, $p<0.0001$. n.s., not significant.

3.3.5 D2 receptor is required for normal learning process

After characterizing the signaling pathway involved in aberrant inhibitory learning, we also studied the signaling pathway required for memory of normal learning. The roles of both D1 and D2 pathways in motor control and learning are well-documented[106]. Interestingly, our experiments with conditional YTHDF1 knockout in the D2 pathway revealed that regulation of protein synthesis—and consequently, normal rotarod learning—is dependent on the D1 pathway rather than the D2 pathway (chapter 2). This suggests that the D1 pathway plays a key role in the consolidation of normal rotarod

memory. Nonetheless, this finding does not dismiss the significance of D2 receptors in the learning process. To explore this, we assessed the motor performance of D2 dopamine receptor knockdown (D2 Kd) mice[107] on standard rotarod learning tasks. We found that the D2 Kd mice displayed significant learning deficits compared to their control counterparts (Figure 3.4B, Two-way ANOVA, group effect, $F(1, 10) = 58.86$, $p < 0.0001$; group x time interaction $F(24, 240) = 1.124$, $p = 0.32$). This outcome underscores the requirement of D2 receptor activity in motor learning and movement regulation, indicating its essential contribution alongside the D1 pathway to normal learning processes. Additionally, D2 receptor on the axonal terminal of dopaminergic neuron and cortical neurons may also contribute to the phenotype in the D2 Kd mice.

3.3.6 Rescue of aberrant inhibitory learning by D1 agonist

With the understanding of neuronal population and signaling pathway underlying normal and aberrant inhibitory learning, we explored potential ways to improve motor performance after aberrant inhibitory learning. Our fiberphotometry *in vivo* recording showed that reduced dSPN activity is associated with poorer rotarod performance, especially during trials where the mice performance lasts less than 5 seconds during the probe phase (chapter 2). We next test whether increasing dSPN activity could counteract aberrant inhibitory learning. To this end, we designed a three-phase experiment involving three groups of mice (illustrated in Figure 3.5A, top). Initially, during the normal learning phase, only one group underwent rotarod training to develop the memory of normal learning. Subsequently, to induce aberrant inhibitory learning, all

groups received a cocktail of D1 and D2 antagonists and were trained on rotarod. The probe phase introduced varied treatments: the group with prior normal learning experience received saline to reflect the preserved memory of normal learning; the remaining groups were administered either a D1 agonist or no treatment to evaluate the potential of D1 agonist in rescuing rotarod performance from aberrant inhibitory learning.

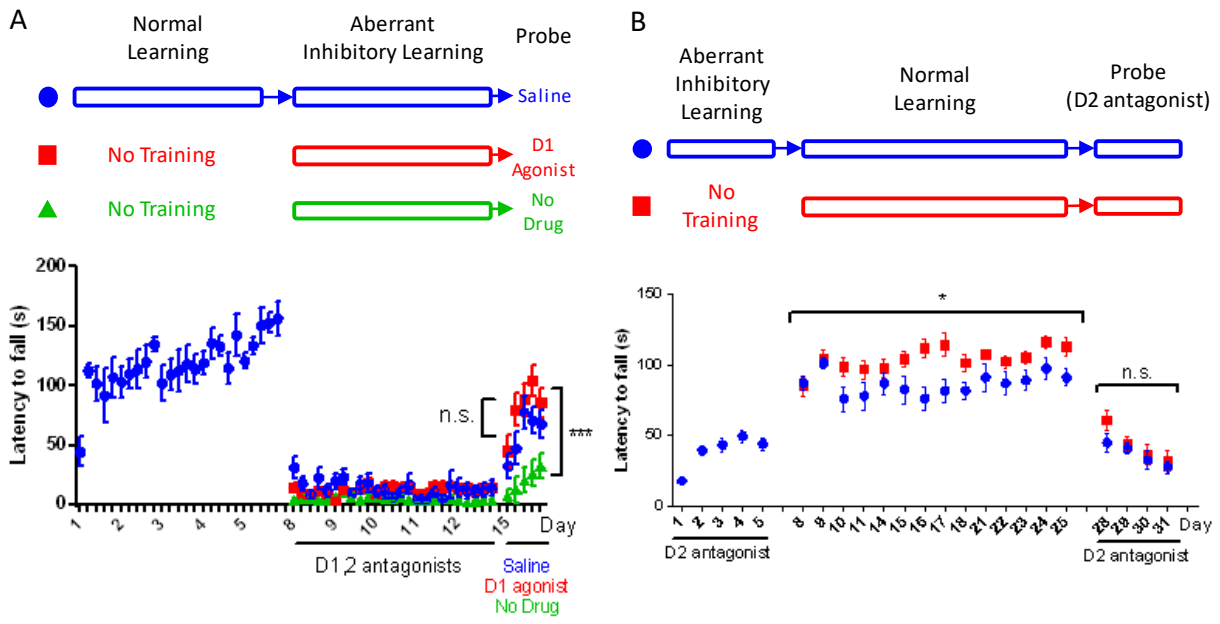

Fig 3.5. Rescue of aberrant inhibitory learning by D1 agonist and prolonged normal learning process.
(A) top, three phase experimental designs for three different groups of mice. Blue group went through normal learning, aberrant inhibitory learning and saline treated probe phase; red group went through aberrant inhibitory learning and D1 agonist SKF treated probe phase; green group went through aberrant inhibitory learning and no drug treated probe phase. bottom, rotarod performance for three different groups. Two-way ANOVA between red and green groups during probe phase, group effect, $F(1, 17) = 16.85$, $p = 0.0007$, group x time interaction $F(4, 68) = 1.28$, $p = 0.29$; Two-way ANOVA between blue and red groups during probe phase, group effect, $F(1, 18) = 2.34$, $p = 0.14$, group x time interaction $F(4, 72) = 0.53$, $p = 0.72$; n(blue group) = 8, n(red) = 12, n(green) =7. (B) top, three phase experimental designs for two groups of mice. Blue group went

Fig 3.5 cont.
through Eticlopride treated aberrant inhibitory learning, normal learning and Eticlopride treated probe phase; red group went through normal learning and Eticlopride treated probe phase; bottom, rotarod performance for the two groups of mice. Two-way ANOVA for normal learning phase (day 8-25), group effect, $F(1, 14) = 6.36$, $p = 0.024$; group x time interaction $F(13, 182) = 1.969$, $p = 0.026$; Two-way ANOVA for probe phase (day 28-31), group effect, $F(1, 14) = 1.48$, $p = 0.243$; group x time interaction $F(3, 42) = 0.638$, $p = 0.595$; n = 8 for each group.
All data represents mean ± SEM. *, $p<0.05$; **, $p<0.01$. n.s., not significant.

Performance during the probe phase showed a significant improvement in rotarod performance in mice treated with the D1 agonist compared to those untreated (Figure 3.5A bottom, Two-way ANOVA between red and green groups during the probe phase, group effect, $F(1, 17) = 16.85$, $p = 0.0007$; group x time interaction $F(4, 68) = 1.28$, $p = 0.29$). Crucially, the performance of the D1 agonist-treated group is similar to the group with prior normal learning experience (Figure 3.5A bottom, Two-way ANOVA between blue and red groups during the probe phase, group effect, $F(1, 18) = 2.34$, $p = 0.14$; group x time interaction $F(4, 72) = 0.53$, $p = 0.72$). This suggests that activation of dSPNs through D1 agonist treatment effectively counteracts the performance deficits resulting from aberrant inhibitory learning.

3.3.7 Erasing aberrant inhibitory learning through normal learning process (WT mice)

With D1 agonist treatment successfully improve the performance after aberrant inhibitory learning, we next test if there are other ways to improve it. In the previous chapter, we demonstrated that aberrant inhibitory learning could be reversed by normal

learning processes in Pitx3 mutant mice. To explore if this reversal is a general phenomenon, we conducted a similar experiment with WT mice. A challenge with WT mice is the acute impairment in rotarod performance following treatment with a cocktail of D1 and D2 antagonists, which prevent us from assessing the reversal of aberrant inhibitory learning post-normal learning. Because of this, we opted to induce aberrant inhibitory learning using solely a D2 antagonist, as reported by our previous results[43]. The experiment divided mice into two groups (Figure 3.5B, top). In the aberrant inhibitory learning phase, one group underwent rotarod training post-D2 antagonist treatment, while the other group, also treated, remained untrained in their cages. Subsequently, both groups received rotarod training without any drug interference during the normal learning phase. The final probe phase involved re-treating both groups with the D2 antagonist to evaluate the reversal of aberrant inhibitory memory.

Consistent with our earlier findings, there was a significant differences between the two groups during the normal learning phase (Figure 3.5B, Two-way ANOVA for normal learning phase (day 8-25), group effect, $F(1, 14) = 6.36$, $p = 0.024$; group x time interaction $F(13, 182) = 1.969$, $p = 0.026$), indicating that D2 antagonist treatment led to lasting aberrant inhibitory memory in the trained mice. Should this aberrant memory be reversible through normal learning, both groups would exhibit comparable performance during the probe phase post-D2 antagonist re-exposure. As predicted, performance between the two groups after extended normal learning mirrored each other, gradually declining over several days (Figure 3.5B, Two-way ANOVA for probe phase (day 28-31), group effect, $F(1, 14) = 1.48$, $p = 0.243$; group x time interaction $F(3, 42) = 0.638$, p

= 0.595). This supports our hypothesis that normal learning processes can indeed reverse aberrant inhibitory memory.

3.4 Discussion

In our study, we observed distinct cFos expression patterns in the M1 and M2 motor cortex between normal and aberrant inhibitory learning, with minimal expression in the striatum. This differential expression correlates with rotarod performance, suggesting cFos as a potential marker for encoding both types of motor memories. This finding aligns with previous research that the immediate early gene Arc in the M2 cortex plays a crucial role in consolidating motor memory engrams, with its expression stabilizing after repeated training sessions[108]. Considering our analysis focused on cFos expression post-memory formation, it would be interesting to map out the cFos expression pattern during the course of motor learning.

While our observations highlight limited cFos activity within the striatum, this does not preclude the striatum's involvement in motor memory storage. Findings from other studies suggest the striatum's important role in motor memory expression[12], indicating a complex interplay between cortical and striatal regions in memory consolidation and retrieval. Given these considerations, future research could benefit from exploring additional immediate early genes, like Arc, to identify the neural networks underlying normal and aberrant motor learning in the striatum, or trying to measure cFos expression at early stage of the learning process. An alternative approach could be

focusing on the projection of cFos positive cells from M1, M2 cortex to the striatum. Such investigations could help us better understand the striatum's contributions alongside cortical regions, offering a more comprehensive understanding of the neural substrates of motor memory.

In our exploration of neuronal populations involved in normal and aberrant inhibitory learning within Pitx3 mutant mice, we found an intriguing trend: the aberrant inhibitory learning group exhibited increased cFos expression in the M2 cortex compared to their normal learning counterparts. This observation suggests a distinct neuronal activation pattern associated with aberrant learning processes. To better understand of these mechanisms, it is important to conduct further research aimed at quantifying the specific cell types—such as excitatory and inhibitory neurons—among the cFos-positive cells. Such analysis will be important for understanding the precise neuronal ensembles that underlie aberrant inhibitory learning. Identifying the cell types of the aberrant motor memory could potentially provide novel targets for therapeutic interventions aimed at mitigating motor deficits in PD.

Dopamine receptors' interaction with Adenylyl cyclase plays a crucial role in regulating intracellular cAMP levels, a key player in neuronal signaling and synaptic plasticity. Our experiments utilized DREADDs to manipulate these cAMP levels, and we found that merely increasing cAMP is insufficient for triggering aberrant inhibitory learning or for consolidating impaired behavior induced by D1 antagonists into long-term memory. These findings point to the involvement of additional mechanisms beyond cAMP-

mediated protein synthesis in the processes underlying aberrant inhibitory learning. It raises the possibility that the role of cAMP-mediated downstream protein synthesis might be to consolidate synaptic changes initiated by dopamine antagonists and behavior learning experience. Future research could explore how cAMP influences the long-term maintenance of corticostriatal synaptic plasticity. Such studies could provide insights into the molecular and synaptic mechanism of learning and memory, offering new perspectives on how synaptic plasticity is maintained over time.

Additionally, some outcomes of our chemogenetic experiments were less definitive than anticipated. Future studies may benefit from localized manipulations: (1) performing local infusion of DREADDs activators to more precisely modulate neuronal activity in the striatum, and (2) using Arc-Cre transgenic mouse lines for the specific labeling of memory engrams associated with both normal and aberrant learning. This approach would enable the expression of chemogenetic proteins directly within these engram cells, allowing for targeted manipulation of the neuronal ensembles across various learning contexts.

In terms of potential treatment for aberrant inhibitory learning, activating the D1 pathway emerges as a promising strategy for mitigating aberrant inhibitory memory, consistent with our fiber photometry findings that link low dSPN activity to impaired rotarod performance. However, it is possible that D1 agonist only acutely activated D1 pathway to mitigate the aberrant inhibitory memory in D2 pathway, and whether this approach induces long-term benefit needs further exploration. Alternatively, our experiments

demonstrate that aberrant inhibitory learning can be effectively reversed by standard rotarod training under conditions of sufficient dopamine level. This aligns with the clinical observations in Parkinson's disease (PD) patients. When under L-DOPA treatment, PD patients showed gradual improvements in motor function. After a period of treatment, they even showed a persistent improvement under no L-DOPA condition, suggesting the reversal of aberrant inhibitory memory. Investigating the mechanisms through which aberrant inhibitory memory is overturned, particularly examining the reversal of D2 receptor-mediated long-term potentiation (LTP), could yield valuable insights for PD treatment strategies.

3.5 Method

3.5.1 Transgenic mice

Several mouse lines used in the experiment were purchased from JAX: A2a-Gαs DREADDs (Jax Strain #:017863), Cre-Gi DREADDs (Jax Strain #026219), β-arrestin 2(Jax Strain #023852), Pitx3 mutant mice (Jax Strain #:000942). A2a-Cre mice were purchased from MMRRC (RRID: MMRRC_036158-UCD). Dopamine D2 receptor knockdown (D2 Kd) mice were previously generated in the lab[107].

3.5.2 Rotarod

Mice in the task are 8-12 weeks old unless otherwise stated. A computer-controlled rotarod apparatus (Rotamex-5, Columbus Instruments, Columbus, OH) with a rat rod

(7cm diameter) was set to accelerate from 4 to 40 revolutions per minute over 300 seconds, and recorded time to fall. Mice received 5 consecutive trials per session, 1 session per day. Rest between trials was approximately 30 seconds.

3.5.3 Open field

Open field chambers were 40 × 40 cm (Med Associates, St. Albans, VT, USA) with lighting at 21 lux. Each chamber was surrounded by black drop cloth obscuring views beyond the chamber. Infrared beams recorded the animals' locomotor activity. Data was collected in 1 min bins during each session. All drugs were administered immediately prior to mice being placed in the open field.

3.5.4 Drug Administration

All drug injections were intraperitoneal at 0.01ml/gram of body weight. L-DOPA (3,4-dihydroxy-L-phenylalanine 25 mg/kg with 12.5mg/kg benserazide) was administered 1 hour prior to the start of each session. SCH 23390 at 0.1mg/kg and eticlopride at 0.16mg/kg were administered 30 minutes prior to experiments. Deschloroclozapine (DCZ) at indicated dose were injected 35 min before the rotarod experiment.

3.5.5 Immunostaining

Brain tissues were fixed with 4% formaldehyde at 1 hour after the rotarod training. Brains were transferred into 30% sucrose for 24 hr, and then 20 μm coronal serial brain sections were made using a cryostat (Leica Instruments). Sections were blocked in TBS

containing 5% normal donkey serum and 0.3% Triton X-100 for 1 h at room temperature, transferred to cFos primary antibody (Cell Signaling, cFos Rabbit #2250) containing 0.3% Triton X-100 with 1% BSA, and incubated at 4°C overnight. Secondary antibodies (Life Technology Invitrogen) were diluted in 5% normal serum at 1:500 for 1 hr at room temperature.

3.5.6 Quantification and statistical analysis

Data are reported as mean ± SEM, and n represents the number of mice used per experiment unless otherwise stated. Statistical analyses were conducted in Graphpad. Statistical significance was assessed using a student's t test or repeated-measures ANOVA for experiments that tracked behavior over time or repeated training. For significant findings after ANOVA, post-hoc Tukey's HSD tests were used to identify specific group differences. The level of significance was set at $p < 0.05$.

CHAPTER 4 DISCUSSION

4.1 Tag and capture in the basal ganglia: A hypothesis

The interplay between normal and aberrant inhibitory learning and the signaling mechanisms that underlie these processes can be simplified through a computational model centered around the 'tag and capture' hypothesis[88]. This hypothesis suggests that the synthesis of new proteins is essential for transforming early long-term plasticity into late long-term plasticity. By integrating this idea with the distinct signaling pathways of D1 and D2 dopamine receptors, our computational model provides insights into the preservation of memory in normal learning after aberrant inhibitory learning and the reversibility of aberrant learning through normal learning processes.

Originally conceptualized in the field of hippocampal research[109,110], the 'tag and capture' hypothesis outlines a two-step mechanism crucial for establishing late long-term synaptic plasticity. Initially, synaptic activity triggers early long-term plasticity (e-LTP) marked by synaptic protein changes that occur independently of new protein synthesis. This e-LTP is transient, gradually reverting to baseline. However, sufficiently potent stimuli activate downstream signaling, prompting the synthesis of proteins like Arc and cFos. These proteins are then transported to or synthesized locally at synapses marked by e-LTP, inducing sustained synaptic structural alterations that underlie late long-term plasticity (l-LTP). Central to this process are the synaptic tags that label the synapses for long-term plasticity, and the mechanisms by which newly synthesized

proteins are 'captured' by these tags. While significant strides have been made in deciphering these molecular processes within the hippocampus, their relevance and application to other brain regions, such as the basal ganglia, remain less understood.

In this final chapter of the thesis, we here propose a framework of ‘tag and capture’ in the basal ganglia, with an addition of the dopamine signaling. We focus on the synaptic plasticity at the corticostriatal synapse, where early long-term plasticity (e-LTP) will be induced by the combination of pre- and post- synaptic activity and dopamine signal[111–113]. In addition to the initial synaptic plasticity, dopamine signal will induce intracellular cAMP-PKA-CREB-protein synthesis pathway to synthesize new protein and will be captured by the synapse undergoing e-LTP. Supported by our behavioral experiments, *in vivo* fiber photometry recordings, chemogenetic interventions, and pharmacological manipulations, this framework elucidates the critical roles of D1 and D2 pathways in normal motor learning and aberrant inhibitory learning, respectively. It posits that dopamine blockade leads to diminished cAMP and protein synthesis in dSPNs, preventing early-LTP consolidation and thereby preserving a prior memory of normal learning. Conversely, heightened cAMP and protein synthesis in iSPNs under dopamine blockade conditions solidify aberrant plasticity into late-LTP, leading to prolonged impairment on motor performance.

Future investigations should aim to investigate the molecular nature of aberrant plasticity. Questions such as the mechanism of D2 LTP *in vivo*, the identity of the synaptic tag within corticostriatal synapses, the molecular signals integrating dopamine

with synaptic activity, and the identity of newly synthesized proteins pivotal for corticostriatal synaptic plasticity, require further exploration. Addressing these questions will not only deepen our understanding of synaptic plasticity but also potentially unveil novel targets for therapeutic intervention in disorders characterized by dysregulated learning and memory processes.

4.2 Direct and indirect pathways mediate positive and negative reward prediction error

Dopaminergic neurons are reported to encode reward prediction error in the brain, with phasic firing increase and decrease encode positive and negative reward prediction error, respectively[22,114]. Given the opposite role of direct and indirect pathways, and the fact that they express different dopamine receptors, these two pathways have long been speculated to respond to positive and negative reward prediction error, respectively. Many studies had been carried out to test the hypothesis.

One popular explanation is that D1 and D2 dopamine receptors have different affinity to dopamine, with D2 showing higher affinity[89]. In this framework, D1 receptor is less occupied at tonic dopaminergic firing condition while D2 receptor is saturated. Thus, when dopamine level increases, the D1 receptor is able to transduce dopamine change into intracellular changes. On the other hand, the D2 receptor responds less because it’s saturated at baseline. When there is tonic decrease in dopaminergic neuron firing, D1 receptor response less because it’s already less occupied at baseline, while D2

receptor response more and convert the activity to intracellular cAMP change. Recent evidence by the Sabatini group measuring downstream cAMP and PKA activity supported this model[85].

In addition to the difference in dopamine receptor affinity, we propose that the downstream 'cAMP-CREB-protein synthesis' signaling could also be an important support for the differential role of D1 and D2 pathway in responding to positive and negative PRE. One important reason is that D1 and D2 dopamine receptors are coupled to Gαs and Gi respectively, so that D1 receptor is positively coupled to Adenylyal cyclase while D2 receptor is negatively coupled[90]. This leads to a complete opposite effect of D1 and D2 receptor signaling. In considering the downstream new protein synthesis important for memory consolidation and potentially for consolidating the synaptic plasticity, we could reason that positive RPE mediated synaptic plasticity will be consolidated into D1 pathway, while negative RPE will be consolidated into D2 pathway. Future research testing on these hypotheses will help us better understand the function of the basal ganglia circuits.

4.3 Increased iSPN activity at movement initiation

One interesting observation during the *in vivo* recording is that iSPNs also showed increased calcium activity at the beginning of the rotarod trials, and iSPNs activity is generally at higher magnitude than dSPNs. This is contrary to the classical rate model and fits with the selection-suppression model (see chapter 1)**.** Given the evidence

showing that the same cortical input neuron can innervate both dSPN and iSPN at the same time, one explanation is that the same cortical input will drive the activity of both dSPN and iSPN at the same time, causing elevated iSPN activity at the movement onset. Because direct and indirect pathways form positive and negative feedback loops through the cortico-striatal-thalamic loop, activating both pathways at the same time will ensure balanced activity of the direct pathway. Otherwise, the direct pathway will quickly lose control through the positive feedback loop.

4.4 Aberrant inhibitory learning vs. extinction learning

Aberrant inhibitory learning is induced under the pathological condition of dopamine loss[43,115]. Our observation that pre-existing memory of normal learning is preserved after the aberrant inhibitory learning process suggested a substantial similarity between aberrant inhibitory learning and extinction learning.

Extinction learning has long been shown to not simply erase previous acquired memory[66,116]. Instead, the extinct behavior showed a rapid renewal during re-exposure to the reinforcer or the original context. To date, extensive research have studied the phenomena of extinction learning in both Pavlovian learning and instrumental learning[66]. Many studies in the extinction of instrumental learning are focused on drug addiction, probably because of the therapeutic potential[117]. One of the influential frameworks for instrumental extinction learning postulates that the Prelimbic cortex - Accumbens core-Ventral pallidum pathway is obligatory for reinstatement whereas an Infralimbic cortex-

Accumbens shell pathway is obligatory for extinction[117,118]. Similar to instrumental extinction learning, in our cFos immunostaining experiments, we showed that primary and secondary motor cortex are involved in normal and aberrant inhibitory motor learning. Further characterization of sub-population involved in normal and aberrant inhibitory learning may provide significant insights in the storage of the two memories.

Additionally, we provide evidence that dorsal striatal direct and indirect pathways are mediating normal and aberrant inhibitory learning, respectively. This dissociation in the neuronal pathway showed another similarity between extinction learning and aberrant inhibitory learning. Several reports showed that D1 receptor activity is involved in renewal of instrumental memory after extinction[119–122], with D1 receptor antagonist blocking the renewal of previous acquired memory, such as alcohol seeking. These results showed consistency with our finding that D1 pathway activity is associated with preserved memory of normal learning. On the other hand, reports showed that blocking D2 receptors facilitated extinction of fearing conditioning memories[123], resembling D2 receptor's role in aberrant inhibitory learning. Overall, these similarities suggest exciting potential to generalize our findings in aberrant inhibitory learning to extinction learning under non-pathological conditions and may provide additional insights on how extinction processes modify pre-acquired memory.

4.5 m6A, synaptic plasticity, and memory consolidation

Our results showed that manipulating m6A reader protein YTHDF1 in either dSPN or

iSPN could prevent the formation of normal and aberrant inhibitory motor memory, respectively. While this manipulation showed great potential for future therapeutic development, we do not fully understand how knocking out YTHDF1 in the dSPN and iSPN affects synaptic plasticity and excitability of these neurons. One potential explanation is that knocking out YTHDF1 in dSPNs affected the excitability of dSPNs and prevented the development of D1 LTP during normal learning, leading to an overall decrease in rotarod performance. On the other hand, knocking out YTHDF1 in iSPNs prevented the consolidation of D2 LTP during aberrant inhibitory learning and prevented the formation of aberrant inhibitory memory. Of note, even though we showed that knocking out YTHDF1 in iSPNs caused no change in normal learning process, it may not necessarily mean that D2 pathway is not involved in normal learning process (for example, D2 LTD), as evidenced by our D2 receptor knock-down experiment in chapter 3. Nevertheless, knocking out or inhibiting YTHDF1 in iSPNs showed as a potential therapeutic target to mitigate PD related aberrant inhibitory learning.

4.6 Conclusion

In this thesis, we explored the complex dynamics of motor memory formation and dysfunction within the basal ganglia, with a focus on Parkinson's Disease (PD). Our results revealed the role of the direct (D1) and indirect (D2) pathways in encoding normal motor memories and aberrant inhibitory learning, respectively. This distinction underscores a complex nature of PD's pathophysiology, where not only the loss of dopaminergic neurons but also the consequent dysregulation between these pathways

contributes to the disease's motor symptoms. Notably, our findings showed that while loss of dopamine induces aberrant inhibitory learning that causes motor impairments, pre-existing normal motor memories remain intact and can be reactivated, offering a new angle for therapeutic interventions. The application of genetic manipulations and chemogenetic approaches further highlighted the potential for selectively targeting these pathways to modify disease outcomes. Ultimately, our study opens new avenues for developing treatments that not only aim to prevent aberrant learning and plasticity, but also to reactivate potential preserved memory of normal learning in PD.

REFERENCE

1. Oldenburg, I.A., and Sabatini, B.L. (2015). Antagonistic but Not Symmetric Regulation of Primary Motor Cortex by Basal Ganglia Direct and Indirect Pathways. Neuron *86*, 1174–1181. 10.1016/j.neuron.2015.05.008.
2. Alexander, G.E., DeLong, M.R., and Strick, P.L. (1986). Parallel organization of functionally segregated circuits linking basal ganglia and cortex. Annu Rev Neurosci *9*, 357–381. 10.1146/ANNUREV.NE.09.030186.002041.
3. Lee, J., Wang, W., and Sabatini, B.L. (2020). Anatomically segregated basal ganglia pathways allow parallel behavioral modulation. Nature Neuroscience 2020 23:11 *23*, 1388–1398. 10.1038/s41593-020-00712-5.
4. Hintiryan, H., Foster, N.N., Bowman, I., Bay, M., Song, M.Y., Gou, L., Yamashita, S., Bienkowski, M.S., Zingg, B., Zhu, M., et al. (2016). The mouse cortico-striatal projectome. Nature Neuroscience 2016 19:8 *19*, 1100–1114. 10.1038/nn.4332.
5. Foster, N.N., Barry, J., Korobkova, L., Garcia, L., Gao, L., Becerra, M., Sherafat, Y., Peng, B., Li, X., Choi, J.H., et al. (2021). The mouse cortico–basal ganglia–thalamic network. Nature 2021 598:7879 *598*, 188–194. 10.1038/s41586-021-03993-3.
6. Haber, S.N. (2003). The primate basal ganglia: parallel and integrative networks. J Chem Neuroanat *26*, 317–330. 10.1016/J.JCHEMNEU.2003.10.003.
7. Aoki, S., Smith, J.B., Li, H., Yan, X., Igarashi, M., Coulon, P., Wickens, J.R., Ruigrok, T.J.H., and Jin, X. (2019). An open cortico-basal ganglia loop allows limbic control over motor output via the nigrothalamic pathway. Elife *8*. 10.7554/ELIFE.49995.
8. Doig, N.M., Moss, J., and Bolam, J.P. (2010). Cortical and Thalamic Innervation of Direct and Indirect Pathway Medium-Sized Spiny Neurons in Mouse Striatum. Journal of Neuroscience *30*, 14610–14618. 10.1523/JNEUROSCI.1623-10.2010.
9. Parker, J.G., Marshall, J.D., Ahanonu, B., Wu, Y.W., Kim, T.H., Grewe, B.F., Zhang, Y., Li, J.Z., Ding, J.B., Ehlers, M.D., et al. (2018). Diametric neural ensemble dynamics in parkinsonian and dyskinetic states. Nature *557*, 177. 10.1038/S41586-018-0090-6.
10. Kravitz, A. V., Freeze, B.S., Parker, P.R.L., Kay, K., Thwin, M.T., Deisseroth, K., and Kreitzer, A.C. (2010). Regulation of parkinsonian motor behaviours by optogenetic control of basal ganglia circuitry. Nature *466*, 622–626. 10.1038/NATURE09159.
11. Lee, H.J., Weitz, A.J., Bernal-Casas, D., Duffy, B.A., Choy, M.K., Kravitz, A. V., Kreitzer, A.C., and Lee, J.H. (2016). Activation of Direct and Indirect Pathway Medium Spiny Neurons Drives Distinct Brain-wide Responses. Neuron *91*, 412–424. 10.1016/j.neuron.2016.06.010.
12. Wolff, S.B.E., Ko, R., and Ölveczky, B.P. (2022). Distinct roles for motor cortical and thalamic inputs to striatum during motor skill learning and execution. Sci Adv *8*, 231. 10.1126/SCIADV.ABK0231.
13. Cui, G., Jun, S.B., Jin, X., Pham, M.D., Vogel, S.S., Lovinger, D.M., and Costa, R.M. (2013). Concurrent activation of striatal direct and indirect pathways during action initiation. Nature *494*, 238–242. 10.1038/NATURE11846.
14. Tecuapetla, F., Jin, X., Lima, S.Q., and Costa, R.M. (2016). Complementary Contributions of Striatal Projection Pathways to Action Initiation and Execution. Cell *166*, 703–715. 10.1016/J.CELL.2016.06.032.
15. Koch, E.T., Sepers, M.D., Cheng, J., and Raymond, L.A. (2022). Early Changes in Striatal Activity and Motor Kinematics in a Huntington's Disease Mouse Model. Movement Disorders *37*, 2021–2032. 10.1002/MDS.29168.
16. Calipari, E.S., Bagot, R.C., Purushothaman, I., Davidson, T.J., Yorgason, J.T., Peña, C.J., Walker, D.M., Pirpinias, S.T., Guise, K.G., Ramakrishnan, C., et al. (2016). In vivo

imaging identifies temporal signature of D1 and D2 medium spiny neurons in cocaine reward. Proc Natl Acad Sci U S A *113*, 2726–2731. 10.1073/PNAS.1521238113/VIDEO-2.
17. Klaus, A., Martins, G.J., Paixao, V.B., Zhou, P., Paninski, L., and Costa, R.M. (2017). The Spatiotemporal Organization of the Striatum Encodes Action Space. Neuron *95*, 1171-1180.e7. 10.1016/j.neuron.2017.08.015.
18. Matamales, M., McGovern, A.E., Mi, J.D., Mazzone, S.B., Balleine, B.W., and Bertran-Gonzalez, J. (2020). Local D2- To D1-neuron transmodulation updates goal-directed learning in the striatum. Science (1979) *367*, 549–555. 10.1126/SCIENCE.AAZ5751.
19. Kwak, S., and Jung, M.W. (2019). Distinct roles of striatal direct and indirect pathways in value-based decision making. Elife *8*. 10.7554/ELIFE.46050.
20. Hikida, T., Yawata, S., Yamaguchi, T., Danjo, T., Sasaoka, T., Wang, Y., and Nakanishi, S. (2013). Pathway-specific modulation of nucleus accumbens in reward and aversive behavior via selective transmitter receptors. Proceedings of the National Academy of Sciences *110*, 342–347. 10.1073/PNAS.1220358110.
21. Schultz, W. (2016). Dopamine reward prediction-error signalling: A two-component response. Preprint at Nature Publishing Group, 10.1038/nrn.2015.26 10.1038/nrn.2015.26.
22. Schultz, W., Dayan, P., and Montague, P.R. (1997). A neural substrate of prediction and reward. Science *275*, 1593–1599. 10.1126/SCIENCE.275.5306.1593.
23. Linden, J., James, A.S., McDaniel, C., and Jentsch, J.D. (2018). Dopamine D2 Receptors in Dopaminergic Neurons Modulate Performance in a Reversal Learning Task in Mice. eNeuro *5*. 10.1523/ENEURO.0229-17.2018.
24. Sala-Bayo, J., Fiddian, L., Nilsson, S.R.O., Hervig, M.E., McKenzie, C., Mareschi, A., Boulos, M., Zhukovsky, P., Nicholson, J., Dalley, J.W., et al. (2020). Dorsal and ventral striatal dopamine D1 and D2 receptors differentially modulate distinct phases of serial visual reversal learning. Neuropsychopharmacology 2020 45:5 *45*, 736–744. 10.1038/s41386-020-0612-4.
25. Kruzich, P.J., and Grandy, D.K. (2004). Dopamine D2 receptors mediate two-odor discrimination and reversal learning in C57BL/6 mice. BMC Neurosci *5*, 1–10. 10.1186/1471-2202-5-12/FIGURES/7.
26. Lee, B., Groman, S., London, E.D., and Jentsch, J.D. (2007). Dopamine D2/D3 Receptors Play a Specific Role in the Reversal of a Learned Visual Discrimination in Monkeys. Neuropsychopharmacology 2007 32:10 *32*, 2125–2134. 10.1038/sj.npp.1301337.
27. Yamaguchi, T., Goto, A., Nakahara, I., Yawata, S., Hikida, T., Matsuda, M., Funabiki, K., and Nakanishi, S. (2015). Role of PKA signaling in D2 receptor-expressing neurons in the core of the nucleus accumbens in aversive learning. Proc Natl Acad Sci U S A *112*, 11383–11388. 10.1073/PNAS.1514731112/SUPPL_FILE/PNAS.201514731SI.PDF.
28. Iino, Y., Sawada, T., Yamaguchi, K., Tajiri, M., Ishii, S., Kasai, H., and Yagishita, S. (2020). Dopamine D2 receptors in discrimination learning and spine enlargement. Nature 2020 579:7800 *579*, 555–560. 10.1038/s41586-020-2115-1.
29. Albin, R.L., Young, A.B., and Penney, J.B. (1989). The functional anatomy of basal ganglia disorders. Trends Neurosci *12*, 366–375. 10.1016/0166-2236(89)90074-X.
30. DeLong, M.R., and Wichmann, T. (2007). Circuits and circuit disorders of the basal ganglia. Arch Neurol *64*, 20–24. 10.1001/ARCHNEUR.64.1.20.
31. Hernádez-López, S., Tkatch, T., Perez-Garci, E., Galarraga, E., Bargas, J., Hamm, H., and Surmeier, D.J. (2000). D2 dopamine receptors in striatal medium spiny neurons reduce L-type Ca2+ currents and excitability via a novel PLC[beta]1-IP3-calcineurin-signaling cascade. J Neurosci *20*, 8987–8995. 10.1523/JNEUROSCI.20-24-08987.2000.

32. Nicola, S.M., James Surmeier, D., and Malenka, R.C. (2000). Dopaminergic modulation of neuronal excitability in the striatum and nucleus accumbens. Annu Rev Neurosci *23*, 185–215. 10.1146/ANNUREV.NEURO.23.1.185.
33. Surmeier, D.J., Ding, J., Day, M., Wang, Z., and Shen, W. (2007). D1 and D2 dopamine-receptor modulation of striatal glutamatergic signaling in striatal medium spiny neurons. Trends Neurosci *30*, 228–235. 10.1016/J.TINS.2007.03.008.
34. Reynolds, J.N.J., and Wickens, J.R. (2002). Dopamine-dependent plasticity of corticostriatal synapses. Neural Netw *15*, 507–521. 10.1016/S0893-6080(02)00045-X.
35. Calabresi, P., Picconi, B., Tozzi, A., and Di Filippo, M. (2007). Dopamine-mediated regulation of corticostriatal synaptic plasticity. Trends Neurosci *30*, 211–219. 10.1016/J.TINS.2007.03.001.
36. Lovinger, D.M. Mini-review Neurotransmitter roles in synaptic modulation, plasticity and learning in the dorsal striatum. Neuropharmacology *58*, 951–961. 10.1016/j.neuropharm.2010.01.008.
37. Shen, W., Flajolet, M., Greengard, P., and Surmeier, D.J. (2008). Dichotomous dopaminergic control of striatal synaptic plasticity. Science (1979) *321*, 848–851. 10.1126/SCIENCE.1160575/SUPPL_FILE/SHEN_SOM.PDF.
38. Surmeier, D.J., Plotkin, J., and Shen, W. (2009). Dopamine and synaptic plasticity in dorsal striatal circuits controlling action selection. Curr Opin Neurobiol *19*, 621–628. 10.1016/J.CONB.2009.10.003.
39. Zhuang, X., Mazzoni, P., and Kang, U.J. (2013). The role of neuroplasticity in dopaminergic therapy for Parkinson disease. Nature Reviews Neurology 2013 9:5 *9*, 248–256. 10.1038/nrneurol.2013.57.
40. Wiecki, T. V., Riedinger, K., Von Ameln-Mayerhofer, A., Schmidt, W.J., and Frank, M.J. (2009). A neurocomputational account of catalepsy sensitization induced by D2 receptor blockade in rats: context dependency, extinction, and renewal. Psychopharmacology (Berl) *204*, 265. 10.1007/S00213-008-1457-4.
41. Wiecki, T. V., and Frank, M.J. (2010). Neurocomputational models of motor and cognitive deficits in Parkinson's disease. Prog Brain Res *183*, 275–297. 10.1016/S0079-6123(10)83014-6.
42. Kreitzer, A.C., and Malenka, R.C. (2007). Endocannabinoid-mediated rescue of striatal LTD and motor deficits in Parkinson's disease models. Nature 2006 445:7128 *445*, 643–647. 10.1038/nature05506.
43. Beeler, J.A., Frank, M.J., McDaid, J., Alexander, E., Turkson, S., Sol Bernandez, M., McGehee, D.S., and Zhuang, X. (2012). A role for dopamine-mediated learning in the pathophysiology and treatment of Parkinson's disease. Cell Rep *2*, 1747–1761. 10.1016/J.CELREP.2012.11.014.
44. Beeler, J.A., Cao, Z.F.H., Kheirbek, M.A., Ding, Y., Koranda, J., Murakami, M., Kang, U.J., and Zhuang, X. (2010). Dopamine-Dependent Motor Learning Insight into Levodopa's Long-Duration Response. Ann Neurol *67*, 639. 10.1002/ANA.21947.
45. Koranda, J.L., Krok, A.C., Xu, J., Contractor, A., McGehee, D.S., Beeler, J.A., and Zhuang, X. (2016). Chronic nicotine mitigates aberrant inhibitory motor learning induced by motor experience under dopamine deficiency. Journal of Neuroscience *36*, 5228–5240. 10.1523/JNEUROSCI.2754-15.2016.
46. Cheung, T.H.C., Ding, Y., Zhuang, X., and Kang, U.J. (2023). Learning critically drives parkinsonian motor deficits through imbalanced striatal pathway recruitment. Proc Natl Acad Sci U S A *120*, e2213093120. 10.1073/PNAS.2213093120/SUPPL_FILE/PNAS.2213093120.SM04.MP4.

47. Bromberg-Martin, E.S., Matsumoto, M., and Hikosaka, O. (2010). Dopamine in motivational control: rewarding, aversive, and alerting. Neuron *68*, 815. 10.1016/J.NEURON.2010.11.022.
48. Iwamoto, T., Okumura, S., Iwatsubo, K., Kawabe, J.I., Ohtsu, K., Sakai, I., Hashimoto, Y., Izumitani, A., Sango, K., Ajiki, K., et al. (2003). Motor dysfunction in type 5 adenylyl cyclase-null mice. J Biol Chem *278*, 16936–16940. 10.1074/JBC.C300075200.
49. Missale, C., Russel Nash, S., Robinson, S.W., Jaber, M., and Caron, M.G. (1998). Dopamine receptors: from structure to function. Physiol Rev *78*, 189–225. 10.1152/PHYSREV.1998.78.1.189.
50. Kheirbek, M.A., Britt, J.P., Beeler, J.A., Ishikawa, Y., McGehee, D.S., and Zhuang, X. (2009). Adenylyl cyclase type 5 contributes to corticostriatal plasticity and striatum-dependent learning. J Neurosci *29*, 12115–12124. 10.1523/JNEUROSCI.3343-09.2009.
51. Matsuoka, I., Suzuki, Y., Defer, N., Nakanishi, H., and Hanoune, J. (1997). Differential expression of type I, II, and V adenylyl cyclase gene in the postnatal developing rat brain. J Neurochem *68*, 498–506. 10.1046/J.1471-4159.1997.68020498.X.
52. Onda, T., Hashimoto, Y., Nagai, M., Kuramochi, H., Saito, S., Yamazaki, H., Toya, Y., Sakai, I., Homcy, C.J., Nishikawa, K., et al. (2001). Type-specific Regulation of Adenylyl Cyclase: SELECTIVE PHARMACOLOGICAL STIMULATION AND INHIBITION OF ADENYLYL CYCLASE ISOFORMS. Journal of Biological Chemistry *276*, 47785–47793. 10.1074/JBC.M107233200.
53. Villacres, E.C., Wu, Z., Hua, W., Nielsen, M.D., Watters, J.J., Yan, C., Beavo, J., and Storm, D.R. (1995). Developmentally expressed Ca2+-sensitive adenylyl cyclase activity is disrupted in the brains of type I adenylyl cyclase mutant mice. Journal of Biological Chemistry *270*, 14352–14357. 10.1074/jbc.270.24.14352.
54. Wu, Z.L., Thomas, S.A., Villacres, E.C., Xia, Z., Simmons, M.L., Chavkin, C., Palmiter, R.D., and Storm, D.R. (1995). Altered behavior and long-term potentiation in type I adenylyl cyclase mutant mice. Proc Natl Acad Sci U S A *92*, 220. 10.1073/PNAS.92.1.220.
55. Impey, S., Wayman, G., Wu, Z., and Storm, D.R. (1994). Type I adenylyl cyclase functions as a coincidence detector for control of cyclic AMP response element-mediated transcription: synergistic regulation of transcription by Ca2+ and isoproterenol. Mol Cell Biol *14*, 8272–8281. 10.1128/MCB.14.12.8272-8281.1994.
56. Augustin, S.M., Beeler, J.A., Mcgehee, D.S., and Zhuang, X. (2014). Cyclic AMP and Afferent Activity Govern Bidirectional Synaptic Plasticity in Striatopallidal Neurons. 10.1523/JNEUROSCI.3906-13.2014.
57. Calabresi, P., Fedele, E., Pisani, A., Fontana, G., Mercuri, N.B., Bernardi, G., and Raiteri, M. (1995). Transmitter release associated with long-term synaptic depression in rat corticostriatal slices. Eur J Neurosci *7*, 1889–1894. 10.1111/J.1460-9568.1995.TB00710.X.
58. Ochi, M., Inoue, H., Koizumi, S., Shibata, S., and Watanabe, S. (1995). Long-term enhancement of dopamine release by high frequency tetanic stimulation via aN-methyl-d-aspartate-receptor-mediated pathway in rat striatum. Neuroscience *66*, 29–36. 10.1016/0306-4522(94)00559-N.
59. Calabresi, P., Saiardi, A., Pisani, A., Baik, J.H., Centonze, D., Mercuri, N.B., Bernardi, G., and Borrelli, E. (1997). Abnormal Synaptic Plasticity in the Striatum of Mice Lacking Dopamine D2 Receptors. Journal of Neuroscience *17*, 4536–4544. 10.1523/JNEUROSCI.17-12-04536.1997.
60. Wood, A.N. (2021). New roles for dopamine in motor skill acquisition: lessons from primates, rodents, and songbirds. J Neurophysiol *125*, 2361–2374. 10.1152/JN.00648.2020/ASSET/IMAGES/LARGE/JN.00648.2020_F003.JPEG.

61. Ruitenberg, M.F.L., van Wouwe, N.C., Wylie, S.A., and Abrahamse, E.L. (2021). The role of dopamine in action control: Insights from medication effects in Parkinson's disease. Neurosci Biobehav Rev *127*, 158–170. 10.1016/J.NEUBIOREV.2021.04.023.
62. Gerfen, C.R. (2022). Segregation of D1 and D2 dopamine receptors in the striatal direct and indirect pathways: An historical perspective. Front Synaptic Neurosci *14*. 10.3389/FNSYN.2022.1002960.
63. Li, H., and Jin, X. (2023). Multiple dynamic interactions from basal ganglia direct and indirect pathways mediate action selection. Elife *12*. 10.7554/ELIFE.87644.
64. Geddes, C.E., Li, H., and Jin, X. (2018). Optogenetic Editing Reveals the Hierarchical Organization of Learned Action Sequences. Cell *174*, 32-43.e15. 10.1016/J.CELL.2018.06.012.
65. McGregor, M.M., and Nelson, A.B. (2019). Circuit Mechanisms of Parkinson's Disease. Neuron *101*, 1042–1056. 10.1016/J.NEURON.2019.03.004.
66. Bouton, M.E., Maren, S., and McNally, G.P. (2021). Behavioral and neurobiological mechanisms of pavlovian and instrumental extinction learning. Physiol Rev *101*, 611. 10.1152/PHYSREV.00016.2020.
67. Quirk, G.J., and Mueller, D. (2008). Neural mechanisms of extinction learning and retrieval. Neuropsychopharmacology *33*, 56–72. 10.1038/SJ.NPP.1301555.
68. Wang, X., Lu, Z., Gomez, A., Hon, G.C., Yue, Y., Han, D., Fu, Y., Parisien, M., Dai, Q., Jia, G., et al. (2013). N6-methyladenosine-dependent regulation of messenger RNA stability. Nature 2013 505:7481 *505*, 117–120. 10.1038/nature12730.
69. Zou, Z., Wei, J., Chen, Y., Kang, Y., Shi, H., Yang, F., Shi, Z., Chen, S., Zhou, Y., Sepich-Poore, C., et al. (2023). FMRP phosphorylation modulates neuronal translation through YTHDF1. Mol Cell *83*, 4304-4317.e8. 10.1016/J.MOLCEL.2023.10.028.
70. Shi, H., Zhang, X., Weng, Y.L., Lu, Z., Liu, Y., Lu, Z., Li, J., Hao, P., Zhang, Y., Zhang, F., et al. (2018). m6A facilitates hippocampus-dependent learning and memory through YTHDF1. Nature 2018 563:7730 *563*, 249–253. 10.1038/s41586-018-0666-1.
71. Luk, K.C., Rymar, V. V., Van Den Munckhof, P., Nicolau, S., Steriade, C., Bifsha, P., Drouin, J., and Sadikot, A.F. (2013). The transcription factor Pitx3 is expressed selectively in midbrain dopaminergic neurons susceptible to neurodegenerative stress. J Neurochem *125*, 932–943. 10.1111/JNC.12160.
72. Liang, B., Zhang, L., Zhang, Y., Werner, C.T., Beacher, N.J., Denman, A.J., Li, Y., Chen, R., Gerfen, C.R., Barbera, G., et al. (2022). Striatal direct pathway neurons play leading roles in accelerating rotarod motor skill learning. iScience *25*, 104245. 10.1016/J.ISCI.2022.104245.
73. Kupferschmidt, D.A., Juczewski, K., Cui, G., Johnson, K.A., and Lovinger, D.M. (2017). Parallel, but Dissociable, Processing in Discrete Corticostriatal Inputs Encodes Skill Learning. Neuron *96*, 476-489.e5. 10.1016/J.NEURON.2017.09.040.
74. Yin, H.H., Mulcare, S.P., Hilário, M.R.F., Clouse, E., Holloway, T., Davis, M.I., Hansson, A.C., Lovinger, D.M., and Costa, R.M. (2009). Dynamic reorganization of striatal circuits during the acquisition and consolidation of a skill. Nat Neurosci *12*, 333. 10.1038/NN.2261.
75. Dieterich, D.C., Lee, J.J., Link, A.J., Graumann, J., Tirrell, D.A., and Schuman, E.M. (2007). Labeling, detection and identification of newly synthesized proteomes with bioorthogonal non-canonical amino-acid tagging. Nature Protocols 2007 2:3 *2*, 532–540. 10.1038/nprot.2007.52.
76. Dieterich, D.C., Hodas, J.J.L., Gouzer, G., Shadrin, I.Y., Ngo, J.T., Triller, A., Tirrell, D.A., and Schuman, E.M. (2010). In situ visualization and dynamics of newly synthesized proteins in rat hippocampal neurons. Nature Neuroscience 2010 13:7 *13*, 897–905. 10.1038/nn.2580.

77. Landgraf, P., Antileo, E.R., Schuman, E.M., and Dieterich, D.C. (2015). BONCAT: Metabolic labeling, click chemistry, and affinity purification of newly synthesized proteomes. Methods in Molecular Biology *1266*, 199–215. 10.1007/978-1-4939-2272-7_14/FIGURES/2.
78. Perrin, E., and Venance, L. (2019). Bridging the gap between striatal plasticity and learning. Curr Opin Neurobiol *54*, 104–112. 10.1016/J.CONB.2018.09.007.
79. Alberini, C.M., and Kandel, E.R. (2015). The Regulation of Transcription in Memory Consolidation. Cold Spring Harb Perspect Biol *7*, a021741. 10.1101/CSHPERSPECT.A021741.
80. Rescorla, R., and Wagner, A.R. (1972). A theory of Pavlovian conditioning : Variations in the effectiveness of reinforcement and nonreinforcement.
81. Bloem, B.R., Okun, M.S., and Klein, C. (2021). Parkinson's disease. The Lancet *397*, 2284–2303. 10.1016/S0140-6736(21)00218-X/ATTACHMENT/04055C61-9DC5-416D-9929-D92B8F68DF58/MMC2.PDF.
82. Kalia, L. V., and Lang, A.E. (2015). Parkinson's disease. The Lancet *386*, 896–912. 10.1016/S0140-6736(14)61393-3.
83. Koller, W.C., Obeso, Olanow, Nutt, Schapira, Dingemanse, Lieberman, Stocchi, Waters, Jenner, et al. (2008). Levodopa for the treatment of Parkinson's disease. N Engl J Med *359*. 10.1056/NEJMCT0800326.
84. Legaria, A.A., Matikainen-Ankney, B.A., Yang, B., Ahanonu, B., Licholai, J.A., Parker, J.G., and Kravitz, A. V. (2022). Fiber photometry in striatum reflects primarily nonsomatic changes in calcium. Nat Neurosci *25*, 1124. 10.1038/S41593-022-01152-Z.
85. Lee, S.J., Lodder, B., Chen, Y., Patriarchi, T., Tian, L., and Sabatini, B.L. (2021). Cell-type-specific asynchronous modulation of PKA by dopamine in learning. Nature *590*, 451–456. 10.1038/S41586-020-03050-5.
86. Yapo, C., Nair, A.G., Clement, L., Castro, L.R., Kotaleski, J.H., and Vincent, P. (2017). Detection of phasic dopamine by D1 and D2 striatal medium spiny neurons. The Physiological Society J Physiol *595*, 24. 10.1113/JP274475.
87. Kida, S. (2012). A Functional Role for CREB as a Positive Regulator of Memory Formation and LTP. Exp Neurobiol *21*, 136. 10.5607/EN.2012.21.4.136.
88. Redondo, R.L., and Morris, R.G.M. (2010). Making memories last: the synaptic tagging and capture hypothesis. Nature Reviews Neuroscience 2011 12:1 *12*, 17–30. 10.1038/nrn2963.
89. Richfield, E.K., Penney, J.B., and Young, A.B. (1989). Anatomical and affinity state comparisons between dopamine D1 and D2 receptors in the rat central nervous system. Neuroscience *30*, 767–777. 10.1016/0306-4522(89)90168-1.
90. Nair, A.G., Gutierrez-Arenas, O., Eriksson, O., Vincent, X., and Kotaleski, J.H. (2015). Cellular/Molecular Sensing Positive versus Negative Reward Signals through Adenylyl Cyclase-Coupled GPCRs in Direct and Indirect Pathway Striatal Medium Spiny Neurons. 10.1523/JNEUROSCI.0730-15.2015.
91. Yapo, C., Nair, A.G., Clement, L., Castro, L.R., Hellgren Kotaleski, J., and Vincent, P. (2017). Detection of phasic dopamine by D1 and D2 striatal medium spiny neurons. Journal of Physiology *595*, 7451–7475. 10.1113/JP274475.
92. Skinbjerg, M., Sibley, D.R., Javitch, J.A., and Abi-Dargham, A. (2011). Imaging the high-affinity state of the dopamine D 2 receptor in vivo: Fact or fiction? 10.1016/j.bcp.2011.09.008.
93. Hunger, L., Kumar, A., and Schmidt, R. (2020). Systems/Circuits Abundance Compensates Kinetics: Similar Effect of Dopamine Signals on D1 and D2 Receptor Populations. 10.1523/JNEUROSCI.1951-19.2019.

94. Marcott, P.F., Mamaligas, A.A., and Ford, C.P. Article Phasic Dopamine Release Drives Rapid Activation of Striatal D2-Receptors. 10.1016/j.neuron.2014.08.058.
95. Hernandez, P.J., Sadeghian, K., and Kelley, A.E. (2002). Early consolidation of instrumental learning requires protein synthesis in the nucleus accumbens. Nat Neurosci *5*, 1327–1332. 10.1038/NN973.
96. Peng, J.Y., and Li, B.M. (2009). Protein synthesis is essential not only for consolidation but also for maintenance and post-retrieval reconsolidation of acrobatic motor skill in rats. Mol Brain *2*, 1–10. 10.1186/1756-6606-2-12/FIGURES/3.
97. Hernandez, P.J., and Abel, T. (2008). The role of protein synthesis in memory consolidation: Progress amid decades of debate. Neurobiol Learn Mem *89*, 293. 10.1016/J.NLM.2007.09.010.
98. Myers, K.M., and Davis, M. (2007). Mechanisms of fear extinction. Mol Psychiatry *12*, 120–150. 10.1038/SJ.MP.4001939.
99. Goodman, J., Gabriele, A., Ornelas, R.A.G., and Packard, M.G. (2022). Behavioral and Neural Mechanisms of Latent Extinction: A Historical Review. Neuroscience *497*, 157–170. 10.1016/J.NEUROSCIENCE.2022.06.001.
100. Wen, K., Shi, Z., Yu, P., Mo, L., Sullere, S., Yang, V., Westneat, N., Beeler, J.A., McGehee, D.S., Doiron, B., et al. (2024). Opposing Motor Memories in the Direct and Indirect Pathways of the Basal Ganglia. bioRxiv, 2024.02.26.582159. 10.1101/2024.02.26.582159.
101. Roth, B.L. (2016). DREADDs for Neuroscientists. Preprint at Cell Press, 10.1016/j.neuron.2016.01.040 10.1016/j.neuron.2016.01.040.
102. Jean-Charles, P.Y., Kaur, S., and Shenoy, S.K. (2017). GPCR signaling via β-arrestin-dependent mechanisms. J Cardiovasc Pharmacol *70*, 142. 10.1097/FJC.0000000000000482.
103. Badreddine, N., Zalcman, G., Appaix, F., Saudou, R., Achard, S., Correspondence, F., Becq, G., Tremblay, N., Dé Ric Saudou, F., and Fino, E. (2022). Spatiotemporal reorganization of corticostriatal networks encodes motor skill learning. CellReports *39*, 110623. 10.1016/j.celrep.2022.110623.
104. Farrell, M.S., Pei, Y., Wan, Y., Yadav, P.N., Daigle, T.L., Urban, D.J., Lee, H.-M., Sciaky, N., Simmons, A., Nonneman, R.J., et al. (2013). A Gαs DREADD Mouse for Selective Modulation of cAMP Production in Striatopallidal Neurons. Neuropsychopharmacology *38*, 854–862. 10.1038/npp.2012.251.
105. Donthamsetti, P., Gallo, E.F., Buck, D.C., Stahl, E.L., Zhu, Y., Lane, J.R., Bohn, L.M., Neve, K.A., Kellendonk, C., and Javitch, J.A. (2020). Arrestin recruitment to dopamine D2 receptor mediates locomotion but not incentive motivation. Mol Psychiatry *25*, 2086. 10.1038/S41380-018-0212-4.
106. Keeler, J.F., Pretsell, D.O., and Robbins, T.W. (2014). Functional implications of dopamine D1 vs. D2 receptors: A 'prepare and select' model of the striatal direct vs. indirect pathways. Neuroscience *282*, 156–175. 10.1016/J.NEUROSCIENCE.2014.07.021.
107. Beeler, J.A., Faust, R.P., Turkson, S., Ye, H., and Zhuang, X. (2016). Low Dopamine D2 Receptor Increases Vulnerability to Obesity Via Reduced Physical Activity, Not Increased Appetitive Motivation. Biol Psychiatry *79*, 887–897. 10.1016/J.BIOPSYCH.2015.07.009.
108. Cao, V.Y., Ye, Y., Mastwal, S., Ren, M., Coon, M., Liu, Q., Costa, R.M., and Wang, K.H. (2015). Motor Learning Consolidates Arc-Expressing Neuronal Ensembles in Secondary Motor Cortex. Neuron *86*, 1385–1392. 10.1016/j.neuron.2015.05.022.
109. Goelet, P., Castellucci, V.F., Schacher, S., and Kandel, E.R. (1986). The long and the short of long-term memory--a molecular framework. Nature *322*, 419–422. 10.1038/322419A0.

110. Martin, S.J., Grimwood, P.D., and Morris, R.G.M. (2000). Synaptic plasticity and memory: an evaluation of the hypothesis. Annu Rev Neurosci *23*, 649–711. 10.1146/ANNUREV.NEURO.23.1.649.
111. Izhikevich, E.M. (2007). Solving the distal reward problem through linkage of STDP and dopamine signaling. Cereb Cortex *17*, 2443–2452. 10.1093/CERCOR/BHL152.
112. Debanne, D., Moreno, A.R., Capogna, M., Louth, E.L., Jørgensen, R.L., Korshoej, A.R., Christian, J., and Sørensen, H. (2021). Dopaminergic Neuromodulation of Spike Timing Dependent Plasticity in Mature Adult Rodent and Human Cortical Neurons. 10.3389/fncel.2021.668980.
113. Xu, H., Perez, S., Cornil, A., Detraux, B., Prokin, I., Cui, Y., Degos, B., Berry, H., de Kerchove d'Exaerde, A., and Venance, L. (2018). Dopamine–endocannabinoid interactions mediate spike-timing-dependent potentiation in the striatum. Nature Communications 2018 9:1 *9*, 1–18. 10.1038/s41467-018-06409-5.
114. Schultz, W. (1986). Responses of midbrain dopamine neurons to behavioral trigger stimuli in the monkey. https://doi.org/10.1152/jn.1986.56.5.1439 *56*, 1439–1461. 10.1152/JN.1986.56.5.1439.
115. Li, J., Dani, J.A., and Le, W. (2009). The role of transcription factor Pitx3 in dopamine neuron development and Parkinson's disease. Curr Top Med Chem *9*, 855–859. 10.2174/156802609789378236.
116. (1927), P.I.P. (2010). Conditioned reflexes: An investigation of the physiological activity of the cerebral cortex. Ann Neurosci *17*, 136. 10.5214/ANS.0972-7531.1017309.
117. Kalivas, P.W., and Volkow, N.D. (2005). The neural basis of addiction: A pathology of motivation and choice. American Journal of Psychiatry *162*, 1403–1413. 10.1176/APPI.AJP.162.8.1403/ASSET/IMAGES/LARGE/P42F5.JPEG.
118. Peters, J., Kalivas, P.W., and Quirk, G.J. (2009). Extinction circuits for fear and addiction overlap in prefrontal cortex. Learn Mem *16*, 279–288. 10.1101/LM.1041309.
119. Bossert, J.M., Poles, G.C., Wihbey, K.A., Koya, E., and Shaham, Y. (2007). Differential Effects of Blockade of Dopamine D1-Family Receptors in Nucleus Accumbens Core or Shell on Reinstatement of Heroin Seeking Induced by Contextual and Discrete Cues. Journal of Neuroscience *27*, 12655–12663. 10.1523/JNEUROSCI.3926-07.2007.
120. Hamlin, A.S., Blatchford, K.E., and McNally, G.P. (2006). Renewal of an extinguished instrumental response: Neural correlates and the role of D1 dopamine receptors. Neuroscience *143*, 25–38. 10.1016/J.NEUROSCIENCE.2006.07.035.
121. Crombag, H.S., Grimm, J.W., and Shaham, Y. (2002). Effect of Dopamine Receptor Antagonists on Renewal of Cocaine Seeking by Reexposure to Drug-associated Contextual Cues. Neuropsychopharmacology 2002 27:6 *27*, 1006–1015. 10.1016/s0893-133x(02)00356-1.
122. Hamlin, A.S., Newby, J., and McNally, G.P. (2007). The neural correlates and role of D1 dopamine receptors in renewal of extinguished alcohol-seeking. Neuroscience *146*, 525–536. 10.1016/J.NEUROSCIENCE.2007.01.063.
123. Ponnusamy, R., Nissim, H.A., and Barad, M. (2005). Systemic blockade of D2-like dopamine receptors facilitates extinction of conditioned fear in mice. Learning & Memory *12*, 399–406. 10.1101/LM.96605.